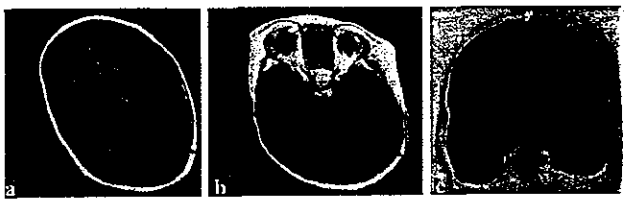

Figure 1. Brain MRI of patient at age 3 years shows agyric frontal and temporo-occipital lobes mixed with pachygyric parietal cortex, hypoplasia of brain stem and cerebellum, and defect of septum pellucidum. The periventricular white matter change (A and B, TR540/TE15; C, TR5400/TE90) also is seen.

pairs were designed to amplify all coding exons and flanking intronic sequences of *POMT1*. The amplified products were sequenced using an ABI PRISM 3100 (Applied Biosystems, Foster City, CA). For the detection and screening of L421del (1260 to 1262 delCCT) in exon 13 of *POMT1*, primers F-CAGTAGCAGCAACTCATGGG, R-ACGGTTGTGGCTGCTATAGC, and restriction enzyme *AvaI* were used. One hundred healthy Japanese individuals served as control subjects.

Results. *Immunohistochemical and immunoblotting analyses.* The immunohistochemical analysis revealed an almost complete loss of immunoreactivity with VIA4-1 anti-α-DG antibody in the patient, whereas anti-α-DG core protein GT20ADG showed membrane staining in each muscle fiber (figure 2). Immunoreaction against the laminin-α2 chain was reduced slightly, but β-DG (see figure 2), dystrophin, and sarcoglycans (not shown) were well preserved.

Immunoblotting analysis using GT20ADG showed a band with a reduced molecular mass, whereas VIA4-1 showed no detectable band for α-DG in the patient (figure 3, A and B). The molecular weight shift observed in our patient (>60 kDa) was almost identical to those reported in FCMD and MEB.[4] On laminin overlay assay, the patient's muscle showed an almost complete loss of laminin-binding activity of α-DG (figure 3C).

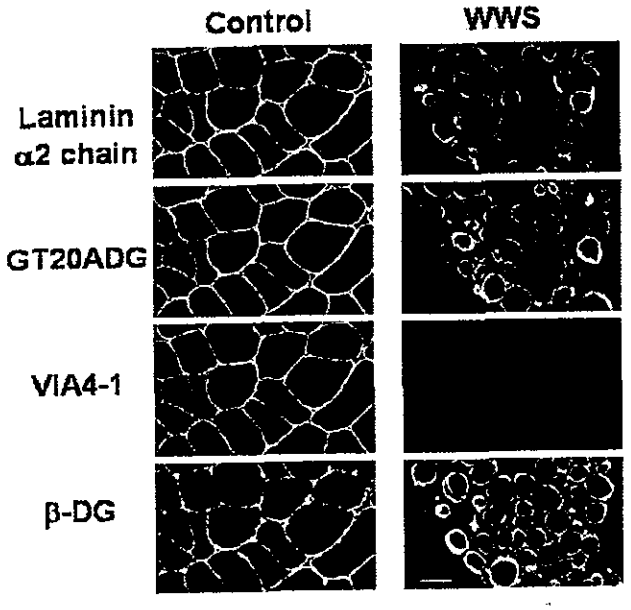

Figure 2. In the patient (with Walker–Warburg syndrome [WWS]), a complete loss of immunoreactivity is observed with the monoclonal antibody VIA4-1 against α-dystroglycan (α-DG), whereas it appears normal around muscle fibers when the polyclonal antibody GT20ADG against α-DG was used. β-DG is well preserved, but the laminin-α2 chain shows mild reduction; bar = 20 μm.

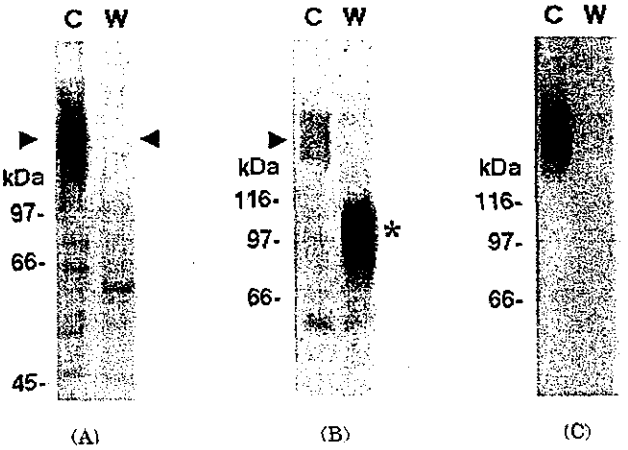

Figure 3. (A) The immunoblotting study using the antibody VIA4-1 showed a broad band around 156 kDa (arrowheads) in control skeletal muscle (C) that is undetectable in the patient (W). (B) The immunoblotting study using the antibody GT20ADG showed a band with a reduced molecular mass (≅90 kDa, asterisk) in the patient, whereas the normal band of α-dystroglycan (α-DG) at 156 kDa was detected in the control. (C) The laminin overlay assay showed loss of band in the patient, suggesting there is an almost complete loss of laminin-binding activity in α-DG from the patient's muscle. M = molecular mass.

Mutation analysis. We found a homozygous deletion of three base pairs (1260 to 1262 delCCT) in *POMT1*, which is expected to delete single amino acid leucine at position 421 (see figure E-1A on the *Neurology* Web site). No identical mutation was present in 100 normal Japanese control subjects (see figure E-1B on the *Neurology* Web site). The amino acid sequence alignment showed that the deleted amino acid leucine and surrounding primary sequence are highly conserved among different species (see figure E-1C on the *Neurology* Web site).

Discussion. In this study, we identified a deletion of the single amino acid leucine at position 421 of *POMT1* from the patient's DNA. This is considered to be a causative mutation for several reasons. First, the same change was not found among 100 Japanese control subjects. Next, the deleted amino acid leucine is located within a highly conserved region of the gene and is conserved among different species. A previously reported V428D mutation also is only seven amino acids downstream to ours.[5] These findings suggest that this conserved region plays an important role in the proper function of the protein.

Our patient showed exceptionally long survival for WWS because most patients with WWS die during infancy and rarely survive beyond age 3

years. Because complete agyria is common in patients with WWS, the pattern of the cortical dysplasia in our patient—agyria mixed with parietal pachygyria in MRI—could be considered milder than typical WWS. Thus, our patient showed intermediate phenotype between WWS and MEB in terms of clinical severity and MRI finding. However, the diagnosis of WWS seems more accurate than MEB or FCMD in our patient because he had a meningoencephalocele, which is almost exclusively seen in WWS.[8] There are some recent reports documenting the remarkable clinical variability originating from the mutation of the same genes causing CMDs, and thus, it is possible for *POMT1* mutations to produce a more benign WWS phenotype like that seen in our patient.[2,3,9]

Although the immunoreactivity against the antibody VIA4-1 was lost completely in our patient, the reaction against the antibody GT20ADG was well preserved. Because the antibody GT20ADG recognizes the core protein of α-DG, our results indicate that α-DG localizes at the surface membrane of skeletal muscle but that the epitope for VIA4-1 antibody was specifically disrupted or masked.[4] Because the antibody VIA4-1 is thought to recognize, at least in part, the carbohydrate epitope of α-DG, the glycosylation status of α-DG is likely to be altered in our patient.[4] The results of immunoblotting and laminin overlay assays further support this speculation. The α-DG from normal skeletal muscle is a heavily glycosylated protein with a molecular weight of 156 kDa. Thus, the reduction of molecular weight, seen only by GT20ADG, is likely to be related to the loss of glycoconjugates from α-DG. Accordingly, the loss of laminin-binding activity shown in the laminin overlay assay most likely is caused by the loss of glycoconjugate, which is thought to be a laminin-binding ligand of α-DG.[6] A brain-selective deletion of dystroglycan in mice was shown recently to cause CMD-like brain malformations and defective laminin binding, giving strong evidence that abnormalities of dystroglycan underlie the neuronal migration disorder seen in this group of disorders.[10] Because similar pattern of glycosylation-deficient disruption of dystroglycan function has been observed in FCMD, MEB, and Large^{myd} mice,[4] it is likely that WWS shares a similar pathomechanism with them. In addition, the complete loss of the laminin-binding activity of α-DG in our patient with WWS is almost identical to that observed in FCMD.[4]

Our study proves that WWS caused by the mutation of *POMT1* coexists with other types of CMDs in the Japanese population. We also demonstrated that WWS is a member of the group of CMDs associated with defective glycosylation of α-DG that results in the loss of function of α-DG as a matrix receptor.

References

1. Muntoni F, Brockington M, Blake DJ, Torelli S, Brown SC. Defective glycosylation in muscular dystrophy. Lancet 2002;360:1419–1421.
2. Taniguchi K, Kobayashi K, Saito K, et al. Worldwide distribution and broader clinical spectrum of muscle-eye-brain disease. Hum Mol Genet 2003;12:527–534.
3. Silan F, Yoshioka M, Kobayashi K, et al. A new mutation of the fukutin gene in a non-Japanese patient. Ann Neurol 2003;53:392–396.
4. Michele DE, Barresi R, Kanagawa M, et al. Post-translational disruption of dystroglycan-ligand interactions in congenital muscular dystrophies. Nature 2002;418:417–422.
5. Beltrán-Valero de Bernabé D, Currier S, Steinbrecher A, et al. Mutations in the O-mannosyltransferase gene POMT1 give rise to the severe neuronal migration disorder Walker-Warburg syndrome. Am J Hum Genet 2002;71:1033–1043.
6. Chiba A, Matsumura K, Yamada H, et al. Structures of sialylated O-linked oligosaccharides of bovine peripheral nerve α-dystroglycan. J Biol Chem 1997;272:2156–2162.
7. Hayashi YK, Ogawa M, Tagawa K, et al. Selective deficiency of alpha-dystroglycan in Fukuyama-type congenital muscular dystrophy. Neurology 2001;57:115–121.
8. Cormand B, Pihko H, Bayes M, et al. Clinical and genetic distinction between Walker-Warburg syndrome and muscle-eye-brain disease. Neurology 2001;56:1059–1069.
9. Topaloglu H, Brockington M, Yuva Y, et al. FKRP gene mutations cause congenital muscular dystrophy, mental retardation, and cerebellar cysts. Neurology 2003;60:988–992.
10. Moore SA, Saito F, Chen J, et al. Deletion of brain dystroglycan recapitulates aspects of congenital muscular dystrophy. Nature 2002;418:422–425.

THE JOURNAL OF BIOLOGICAL CHEMISTRY
Vol. 279, No. 12, Issue of March 19, pp. 11402–11407, 2004
Printed in U.S.A.
© 2004 by The American Society for Biochemistry and Molecular Biology, Inc.

Reduction of UDP-*N*-acetylglucosamine 2-Epimerase/*N*-Acetylmannosamine Kinase Activity and Sialylation in Distal Myopathy with Rimmed Vacuoles*

Received for publication, December 3, 2003, and in revised form, December 30, 2003
Published, JBC Papers in Press, January 5, 2004, DOI 10.1074/jbc.M313171200

Satoru Noguchi‡§¶, Yoko Keira‡§, Kumiko Murayama‡, Megumu Ogawa‡§, Masako Fujita‡§, Genri Kawahara‡§, Yasushi Oya‖, Masaoki Imazawa, Yu-ichi Goto‡‡, Yukiko K. Hayashi‡, Ikuya Nonaka‖, and Ichizo Nishino‡§**

*From the ‡Department of Neuromuscular Research, **Division of Radiation Protection, ‡‡Department of Mental Retardation and Birth Defect Research, National Institute of Neuroscience, and ‖National Center Hospital for Mental, Nervous, and Muscular Disorders, National Center of Neurology and Psychiatry, 4-1-1 Ogawahigashi, Kodaira, Tokyo 187-8502, Japan and §Core Research for Evolutional Science and Technology (CREST), Japan Science and Technology Corporation, Kawaguchi, Saitama 332-0012, Japan*

Distal myopathy with rimmed vacuoles is an autosomal recessive muscle disease with preferential involvement of the tibialis anterior that spares the quadriceps muscles in young adulthood. In a Japanese patient with distal myopathy with rimmed vacuoles, we identified pathogenic mutations in the gene encoding the bifunctional enzyme UDP-GlcNAc 2-epimerase/ManNAc kinase, which catalyzes the initial two steps in the biosynthesis of sialic acid. In this study, we demonstrated the relationship between the genetic mutations and enzymatic activities using an *in vitro* expression assay system. Furthermore, we also showed that the levels of sialic acid in muscle and primary cultured cells from DMRV patients were reduced to 60–75% of control. The reactivities to lectins were also variable in some myofibers, suggesting that hyposialylation and abnormal glycosylation in muscles may contribute to the focal accumulations of autophagic vacuoles, amyloid deposits, or both in patient muscle tissue. The addition of ManNAc and NeuAc to primary cultured cells normalized sialylation levels, thus demonstrating the therapeutic potential of these compounds for this disease.

Distal myopathy with rimmed vacuoles (DMRV)[1] is an autosomal recessive disorder characterized clinically by the preferential involvement of the tibialis anterior muscle, sparing the quadriceps muscles as originally described in 1981 (1, 2). The age at onset is relatively late with a mean of 26 years. Muscle biopsy of this disorder is characterized by many rimmed vacuoles, which are particularly abundant in atrophic fibers. Necrotic and regenerating fibers are rarely seen (3). The nucleus occasionally contains tubulofilamentous inclusions of 15–20 nm in diameter.

Hereditary inclusion body myopathy (HIBM) is an autosomal recessive disorder that presents with adult-onset slowly progressive distal and proximal weakness and has characteristic pathological features in muscle tissue, including rimmed vacuoles and filamentous inclusions, that are similar to those seen in DMRV (4). Gene loci of both diseases have been mapped to chromosome 9 (5, 6). HIBM is caused by mutations in the UDP-GlcNAc 2-epimerase/ManNAc kinase gene (*GNE* gene) (7). Previously we identified homozygous and compound heterozygous mutations in the *GNE* gene in 27 DMRV patients (8), demonstrating that the two diseases are allelic.

UDP-GlcNAc 2-epimerase/ManNAc kinase is a dual functional enzyme catalyzing two initial steps in the biosynthesis of sialic acid (9). This enzyme catalyzes the conversions of UDP-GlcNAc to ManNAc and ManNAc to ManNAc 6-phosphate. Despite the identification of the *GNE* gene mutations, we still do not fully understand how these mutations contribute to the pathophysiology in DMRV/HIBM. Several questions remain unanswered. 1) What is the status of sialylation activity in the patients with *GNE* mutations? One would expect sialylation to be impaired but not completely absent in DMRV/HIBM patients, because sialic acid is essential for embryonic development (10). In fact, homozygous null mutations have never been identified in patients (8, 11). 2) Why are symptoms restricted to the skeletal muscles? *GNE* transcripts are expressed in various tissues and are especially predominant in the liver (12). 3) Why do mutant proteins not complement each other in patients who have heterozygous mutations in each of the two domains? The two domains in GNE protein have been reported to catalyze the enzymatic reactions separately and independently (13). To address these questions, we studied the relationships between mutations and enzymatic activity using *in vitro* expression and enzymatic assay systems. We also determined the levels of sialylation in sera, muscles, and primary cultured cells from DMRV patients and normal individuals.

EXPERIMENTAL PROCEDURES

Mutation and Sialic Acid Analyses of Patients—All of the patients were Japanese. The patients were diagnosed as having DMRV based on both clinical features and muscle pathology. Numbering of the patients followed the protocol presented in our previous report (8). Gene analyses of DMRV patients were performed as described previously (8). Primary fibroblasts were obtained from patient 18 and patient 19, whose mutations were reported previously. Primary skeletal myocytes were obtained from patient 5 as reported previously. Sialic acid contents in sera were measured with a SIALIZYME-550 kit (Fujirevio, Tokyo, Japan), and those in muscle and cells were determined by the

* This study was supported by a grant for research on psychiatric and neurological diseases and mental health. The costs of publication of this article were defrayed in part by the payment of page charges. This article must therefore be hereby marked "*advertisement*" in accordance with 18 U.S.C. Section 1734 solely to indicate this fact.

¶ To whom correspondence should be addressed. Tel.: 81-423412712; Fax: 81-423461742; E-mail: noguchi@ncnp.go.jp.

[1] The abbreviations used are: DMRV, distal myopathy with rimmed vacuoles; HIBM, hereditary inclusion body myopathy; MAM, *Maackia amurensis* lectin; MBS, *m*-maleimidobenzoyl-*N*-hydroxysuccinimido ester; SSA, *Sambucus sieboldiana* agglutinin; SBA, soybean agglutinin; GNE, UDP-GlcNAc 2-epimerase/ManNAc kinase; WGA, wheat germ agglutinin.

This paper is available on line at http://www.jbc.org

thiobarbituric acid method. Informed consents were obtained from all subjects using a form approved by the Ethical Review Board at the National Center of Neurology and Psychiatry (Tokyo, Japan).

Expression of Recombinant GNE Proteins—The cDNA for wild-type *GNE* was obtained by reverse transcribed-PCR from normal muscle RNA and cloned into pCR-blunt vector (Invitrogen). The cDNAs for *GNE* mutants were obtained by reverse transcribed-PCR from skeletal muscle RNA of DMRV patients or by site-directed mutagenesis from wild-type cDNA. All cloned muscle cDNAs were sequenced by ABI cycle-sequencing procedures using an *ABI 3100* (Applied Biosystems, Foster City, CA). The sequenced and inserted cDNAs were cut out with EcoRI and blunted, and the purified cDNA fragments were inserted in-frame into the expression vector, pCMV-Myc (Invitrogen). The expression constructs were transiently transfected into COS-7 cells using LipofectAMINE Plus (Invitrogen) according to the manufacturer's protocol. After 24 h, the Myc-tagged wild-type GNE and the mutant proteins were extracted from transfected cells. UDP-GlcNAc 2-epimerase activity was measured as described previously. The ManNAc kinase assay was performed with slight modification according the previous report (13).

Cross-linking of GNE Mutant Proteins—To analyze the oligomer structure of wild-type and mutant GNE, cell lysates were subjected to a reaction with 10 mM MBS for 30 min at room temperature for cross-linking. The Myc-tagged cross-linked products were purified with anti-Myc-agarose (Santa Cruz Biotechnology, Santa Cruz, CA) and eluted by boiling in 2% SDS solution. The products were subjected to SDS-PAGE and Western blot using anti-Myc *9E10* antibody (Santa Cruz Biotechnology).

Lectin Staining and Protein Analysis of Skeletal Muscles from Patients—Biotin-labeled *Maackia amurensis* (MAM), soybean agglutinin (SBA), and *Sambucus sieboldiana agglutinin* (SSA) (Seikagaku Kogyo, Tokyo, Japan) and fluorescein isothiocyanate-labeled streptavidin (Vector Laboratories, Burlingame, CA) were used for the staining of muscle sections. Unfixed 10-μm-thick muscle sections were blocked in 2% casein/phosphate-buffered saline and stained with lectin solution for 2 h at room temperature. The proteins were extracted from the skeletal muscle sections using 8.5 M urea, 0.5% Nonidet P-40 and analyzed by two-dimensional PAGE. Monoclonal antibodies, H4A3 (for LAMP-1), 43DAG1/8D5 (for β-dystroglycan), and VIA4-I (for α-dystroglycan) were used for Western blotting. Laminin binding to α-dystroglycan was examined as described previously (14).

Cell Cultures—COS-7 cells were cultured in 10% fetal bovine serum/Dulbecco's modified Eagle's medium in 5% CO_2. Primary fibroblasts and myoblasts from DMRV patients and normal individuals were cultured in 10% fetal bovine serum, Dulbecco's modified Eagle's medium, and Ham's F-12 medium in 5% CO_2. The myoblasts were induced to myogenic differentiation by switching the medium to 5% horse serum, Dulbecco's modified Eagle's medium, and Ham's F-12 medium. At 24 h before lectin staining or sialic acid determination, the medium was replaced with serum-free Dulbecco's modified Eagle's medium and Ham's F-12 medium with or without 5 mM GlcNAc, ManNAc, or NeuAc. Cells were fixed and permeabilized as described previously (15). Biotin-labeled SBA, wheat germ agglutinin (WGA) (Seikagaku Kogyo), an antibody against desmin (ICN Pharmaceuticals, Costa Mesa, CA), and Alexa Fluo 594-labeled secondary antibodies (Molecular Probes, Eugene, OR) were used for staining the cells.

RESULTS

Novel Mutations in GNE Gene in DMRV Patients—In the previous study, we identified 12 different *GNE* mutations in either homozygous or compound heterozygous states in 27 DMRV patients (8). From these results, we concluded that DMRV is allelic to HIBM. Subsequently, we identified six patients harboring five different mutations, of which three were novel mutations: 1622C→T, 89G→C, and 2173G→A (Table I). These novel mutations were absent in 100 control chromosomes from normal Japanese individuals.

Enzymatic Activities of GNE Mutants in DMRV Patients—Site-directed mutagenesis of the GNE protein has shown that the two enzymatic activities are separately and independently catalyzed by two domains, an N-terminal epimerase domain and a C-terminal kinase domain (13). Previously, we reported reductions in UDP-GlcNAc 2-epimerase activities in leukocytes from the patients with mutations in the *GNE* gene (8). However, the enzyme activity was too weak in leukocytes to clearly demonstrate correlations between gene mutations and the enzymatic activities. To clarify this relationship, we generated recombinant proteins with each of the 13 species of mutations that we identified. All but one of the mutant and wild-type recombinant GNE proteins were expressed in COS cells and migrated at 75 kDa in SDS-PAGE. The single exception was a recombinant protein with a deletion of amino acids 206–256 (Δ206–256) caused by exon 4 skipping. The abnormal protein was degraded in COS cells (Fig. 1*A*). We determined the specific activities of UDP-GlcNAc 2-epimerase and ManNAc kinase of the mutant proteins relative to wild type (Fig. 1*B*). The endogenous activities in mock transfected COS cells were determined to correct for the background enzyme activity. UDP-GlcNAc 2-epimerase activities in mutants C13S, H132Q, D176V, D177C, V331A, and D378Y were reduced to less than 20% of the control. In contrast, the I472T and G708S mutants each revealed an ~50% reduction, and V572L, A630T, and A631V each showed only a 20–30% reduction in activity as compared with wild-type cells. ManNAc kinase activity was retained in the N-terminal mutants C13S, H132Q, D176V, D177C, V331A, and D378Y, whereas the C-terminal mutants I472T, V572L, A630T, A631V, and G703S showed dramatic reductions in activities. These data were essentially compatible with a prior report (13). Interestingly, the A524V mutant preferentially affected UDP-GlcNAc 2-epimerase activity, although the mutation is in the kinase domain. None of the DMRV mutants showed complete loss of UDP-GlcNAc 2-epimerase or ManNAc kinase activities.

TABLE I
Identified mutations

The mutations were identified in patients diagnosed as having DMRV based on both clinical features and muscle pathology. Numbering of patients followed that in our previous report (8). Exon indicates the exon number where mutation was found. Protein domain is predicted ones from the sequence homology as previously (13).

Patient	Mutation	Exon	Predicted amino acid alteration	Protein domain
28	578A→T	E3	D176V	Epimerase
	1765G→C	E10	V572L	Kinase
29	578A→T	E3	D176V	Epimerase
	578A→T	E3	D176V	Epimerase
30	578A→T	E3	D176V	Epimerase
	1622C→T	E9	A524V	Kinase
31	89G→C	E2	C13S	Epimerase
	89G→C	E2	C13S	Epimerase
32	578A→T	E3	D176V	Epimerase
	2173G→A	E12	G708S	Kinase
33	1765G→C	E10	V572L	Kinase
	1765G→C	E10	V572L	Kinase

Oligomerization of GNE Mutants—GNE protein forms a homohexamer by oligomerization (13). We examined whether the mutations affect the oligomerization of GNE molecules, because homohexamer structure of GNE protein was reported to be essential for UDP-GlcNAc 2-epimerase activity (13). The recombinant mutant proteins were subjected to the cross-linking with MBS. Fig. 1*C* shows the electrophoretic tracing patterns of cross-linked products of wild-type and mutant GNE proteins. The product of wild-type GNE predominantly migrated at >400 kDa, which corresponds to homohexamer. C13S, V572L, A630T, and A631V gave cross-linked products similar to that of wild-type GNE, whereas the mutants H132Q and D176V mainly generated a 200-kDa product, and D177C, V331A, D378Y, and A524V produced 98-kDa proteins. These data indicate that the hexameric oligomerization is necessary for UDP-GlcNAc 2-epimerase activity and that N-terminal mutants generally fail to form large oligomers although the molecular region responsible for the oligomerization is not clearly

TABLE II

The list of their mutations, GNE activities, and the results of lectin staining of patients used in this study

The muscle specimens from patients 5 and 8, the fibroblasts from patients 18 and 19, and the myotubes from patient 5 were used in this study. ND, not determined.

Patient	Mutation	Predicted amino acid alteration	GNE activity[a]	MNK activity[b]	SSA staining in skeletal muscle	SBA staining in skeletal muscle	WGA staining in cultured cell	SBA staining in cultured cell
			%	%				
5	IVS4+4A→G	Exon 4 skipping	ND	ND	Variable	Positive in atrophic fibers	Negative in plasma membrane	Positive
	1765G→C	V572L	68.2	8.3				
8	578A→T	D176V	18.2	86.5	Variable	Positive in atrophic fibers	ND	ND
	1043T→C	V331A	16.1	114				
18	578A→T	D176V	18.2	86.5	ND	ND	Weak	Positive
	1466T→C	I472T	47.5	4.7				
19	578A→T	D176V	18.2	86.5	ND	ND	Weak	Positive
	578A→T	D176V	18.2	86.5				

[a] GNE activity represents UDP-GlcNAc 2-epimerase activity.
[b] MNK activity represents ManNAc kinase activity as percentage relative to that of wild type GNE.

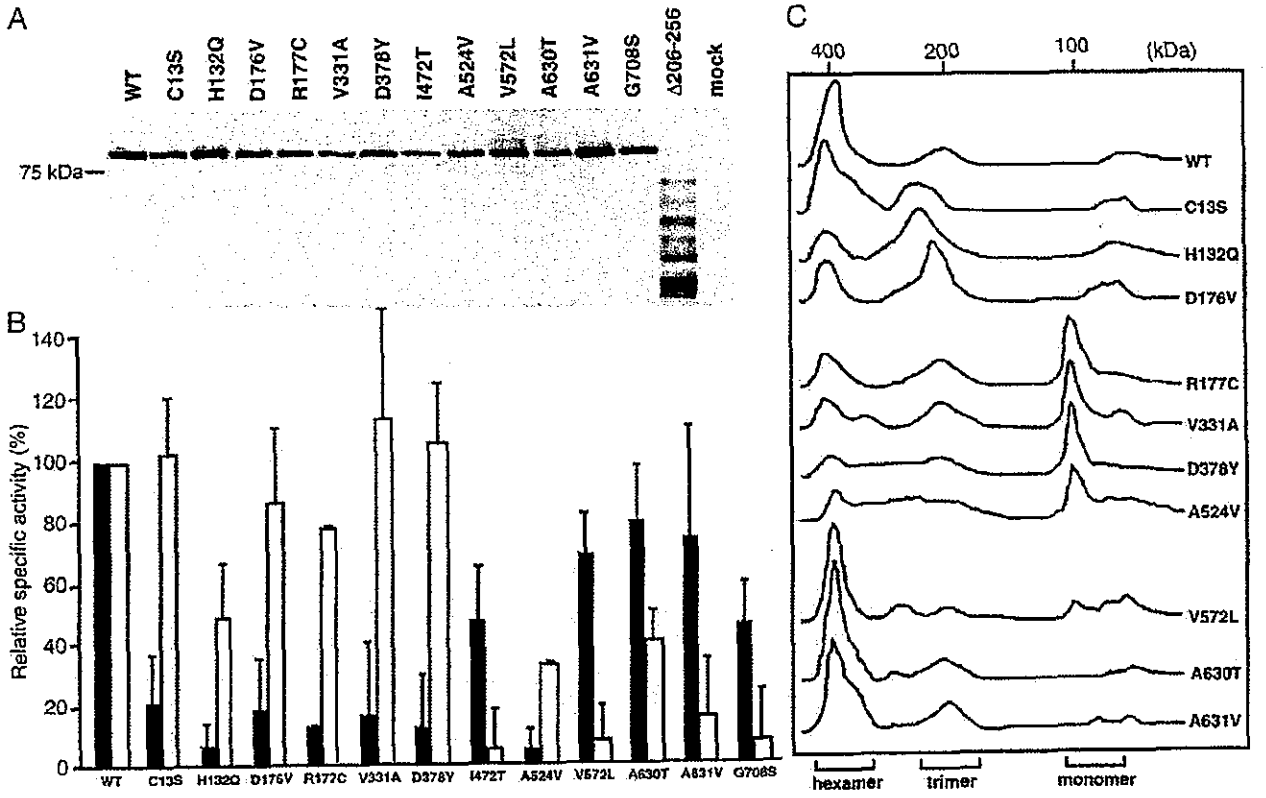

FIG. 1. **Enzymatic activities and oligomerization of mutant GNE proteins.** *A*, Myc-tagged wild-type (*WT*) and mutant GNE proteins expressed in COS cells were separated in SDS-PAGE and Western blotted with anti-Myc antibody. Only the mutant protein with the deletion of amino acids 206–256 was degraded in the cells. *B*, UDP-GlcNAc 2-epimerase (*black*) and ManNAc kinase (*white*) activities were measured *in vitro*. The *bar graphs* display relative specific activities presented as percentage of wild-type activities. *C*, wild-type and mutant GNE proteins were cross-linked with MBS and analyzed by immunoblotting. The immunoreactive patterns of cross-linked products were shown. The predicted migration positions of hexamer, trimer, and monomer are represented at the *bottom*.

related to the predicted oligomerization domains based on the primary structure.

Sialic Acid Contents in Skeletal Muscles and Primary Cells from DMRV Patients—*GNE* gene mutations reduced the enzymatic activity of GNE protein. These results led us to hypothesize that sialylation should be affected in the tissues of DMRV patients. We measured the sialic acid content in sera and muscles from DMRV patients (Fig. 2*A*). In sera, no difference was detected between patients and normal controls, whereas in skeletal muscle, a 25% reduction of sialic acid was observed in DMRV muscles. We also assessed the status of sialylation in DMRV muscles by lectin staining. We used three lectins: SSA for detection of Siaα2–6Gal/GalNAc, MAM for Siaα2–3Gal, and SBA for GalNAcα1–3Gal (16–18) (Fig. 2*B*). The results of lectin staining are summarized in Table II. SSA uniformly stained sarcolemma in control muscle, whereas it faintly stained sarcolemma and strongly stained interstitial tissues in DMRV muscle (Fig. 2*B*, *panels d–f*). MAM strongly stained sarcolemma and interstitial tissues in both the control and patient muscles. We did not observe any reduction in MAM staining in

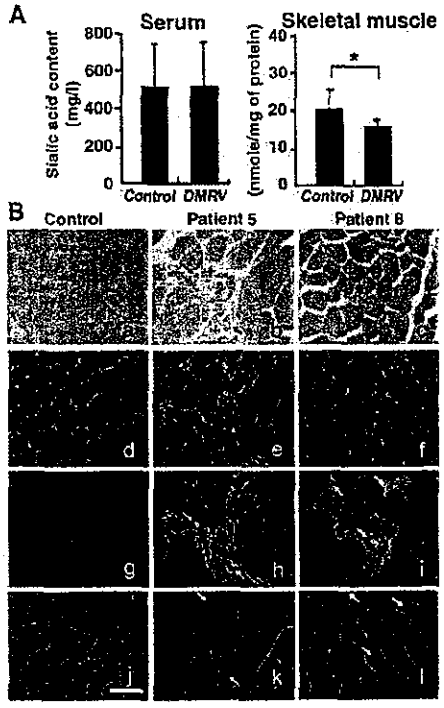

FIG. 2. **Sialylation of sera and muscles from DMRV patients and controls.** *A*, sialic acid contents of the serum from control ($n = 7$) and DMRV patients ($n = 9$, patients 4, 5, 6, 7, 12, 13, 17, 26, and 28) were measured using a *SIALIZYME-550 kit. The sialic acid contents* of muscles from the control ($n = 7$) and DMRV patients ($n = 4$, patients 5, 8, 9, and 13) were measured by the thiobarbituric acid method. *, $p < 0.05$. *B*, lectin staining and immunohistochemical staining of α-dystroglycan in skeletal muscles from control (*a*, *d*, *g*, and *j*) and DMRV patients 5 (*b*, *e*, *h*, and *k*) and patient 8 (*c*, *f*, *i*, and *l*). *a–c*, stained with hematoxylin and eosin; *d–f*, stained with SSA lectin; *g–i*, stained with SBA lectin; *j–l*, stained with an antibody for α-dystroglycan (VIA4-1). *Arrows* indicate rimmed vacuoles. SBA lectin strongly stained sarcolemma and cytoplasmic areas in the cluster of atrophic or rimmed vacuoles containing myofibers.

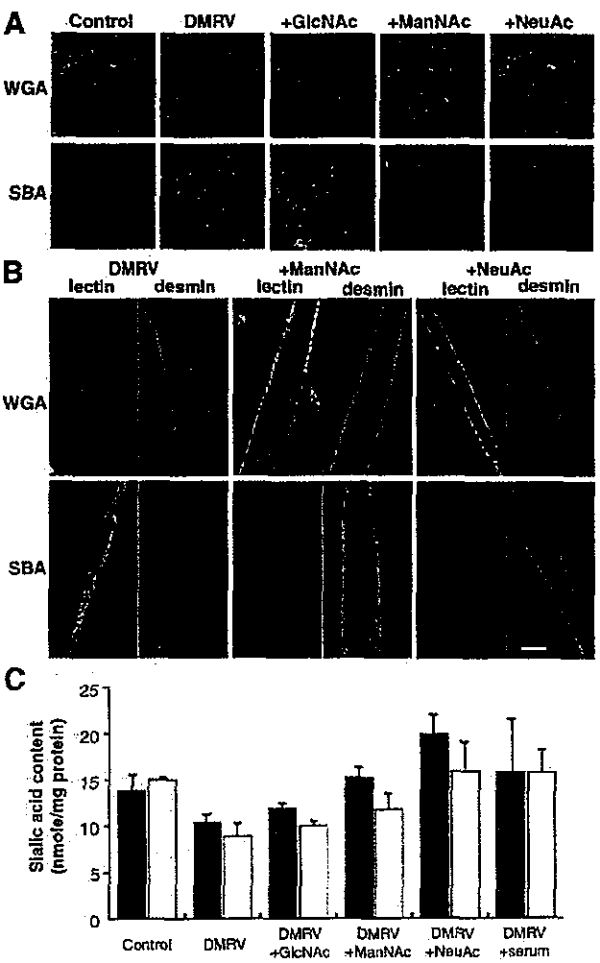

FIG. 3. **Recovery of the *sialylation in* DMRV cells by treatment with ManNAc and NeuAc.** *A*, the fibroblasts from patient 18 (DMRV) and control individuals were stained with WGA and SBA lectins. The patient 18 fibroblasts cultured in the presence of GlcNAc (*+GlcNAc*), ManNAc (*+ManNAc*) and NeuAc (*+NeuAc*) were also stained with both lectins. *B*, differentiated myotubes from patient 5 cultured *without (DMRV)* and with ManNAc (*+ManNAc*) and NeuAc (*+NeuAc*) were stained by WGA and SBA lectins and desmin antibody. Desmin-positive cells are myotubes. *C*, sialic acids in myotubes ($n = 4$ from patient 5, *black*) and fibroblasts ($n = 4$ from patients 18 and 19, *white*) were measured by the thiobarbituric acid method.

patients, which may be attributed to the strong intensity in our staining condition (*data not shown*). In contrast, SBA strongly highlighted the rimmed vacuoles containing fibers and the surrounding atrophic fibers in the patients both in sarcolemma and cytoplasm (Fig. 2*B*, *panels h* and *i*; see *arrows*), whereas it did not stain myofibers in the control (Fig. 2*B*, *panel g*). These data suggest that sialylation, other glycosylation, or both are at least partly disturbed in some myofibers in DMRV. Furthermore, we examined the expression of glycosylated α-dystroglycan in DMRV muscles using an antibody (VIA4-I) that recognizes a carbohydrate epitope. The α-dystroglycan staining was negative in rimmed vacuoles containing fibers and the surrounding atrophic fibers in one DMRV patient (Fig. 2*B*, *panel l*). However, positive staining in another patient demonstrated that α-dystroglycan expression varies among patients (Fig. 2*B*, *panel k*). Therefore, we concluded that the loss of α-dystroglycan staining is an extreme down-stream phenomenon in DMRV muscles. We also analyzed muscle sialylated glycoproteins (LAMP-1, and α- and β-dystroglycans) by one- or two-dimensional polyacrylamide gel electrophoresis, but when they were extracted in whole amounts, there was no significant change in the electrophoretic patterns of these proteins between control and patients (data not shown). Furthermore, we analyzed the laminin-binding property of α-dystroglycan from DMRV patients, and the α-dystroglycan showed a strong binding as the control (data not shown).

Restoration of Sialylation in DMRV Cells by Feeding with ManNAc and NeuAc—Previous studies reported that hyposialylation in *GNE−/−* embryonic stem cells and *GNE*-defective cells can be repaired by feeding with the natural sialic acid precursor ManNAc (10, 19). We examined the recovery of sialylation by the addition of NeuAc or ManNAc using primary cultured cells from patients and evaluated the sialylation status by lectin staining (Fig. 3*A*). We used two lectins, WGA, which specifically recognizes a cluster structure of sialic acids (20), and SBA. WGA strongly stained the perinuclear region in control fibroblasts. Fibroblasts from patient 18, who harbors compound heterozygous missense mutations D176V and I472T, showed weaker staining with WGA compared with normal controls (Fig. 3*A*; *WGA*, *DMRV*, and *Control*). SBA did not stain the fibroblasts from normal controls but strongly stained cells from DMRV patients. These results were also confirmed in myotubes from another DMRV patient (patient 5) who has compound heterozygous mutations causing exon 4 skipping and V572L (Fig. 3*B*) and fibroblasts from patient 19 with a homozygous D176V mutation (data not shown). The sialic acid

levels in skin fibroblasts and myotubes from DMRV patients were significantly decreased at ~60–74% of control cells when cells were cultured in serum-free medium (Fig. 3*C*). By adding ManNAc or NeuAc into the culture medium, sialic acid levels in the fibroblasts and myotubes were restored to normal levels (Fig. 3*C*, *+ManNAc* and *+NeuAc*). Furthermore, WGA staining of cells from patients also increased to normal levels, and particularly strong WGA staining was observed in the plasma membrane of myotubes. In contrast, the SBA staining in DMRV cells disappeared by the addition of either sugar (Fig. 3, *A* and *B*; *+ManNAc* and *+NeuAc*). The addition of GlcNAc into the medium had no effect on the staining pattern with either lectin (Fig. 3, *A* and *C*, *+GlcNAc*). These results suggest the potential therapeutic use of ManNAc and NeuAc.

DISCUSSION

In this study, we identified six additional DMRV patients with *GNE* mutations. Combined with prior results, the 1765G→C mutation accounts for 55% (36 of 66) of the abnormal alleles confirming the high frequency of this mutation in Japan. Haplotype analysis suggests that this common mutation is due to a founder effect (8). All of the mutations identified in DMRV patients caused reduction (but not total loss) of enzymatic activities of either UDP-GlcNAc 2-epimerase or ManNAc kinase. These results strongly suggest that DMRV is caused by partial loss of function of the gene product. Interestingly, we previously identified the compound heterozygous mutations D378Y and A631V in a North American DMRV patient of German and Irish origin; these mutations have also been identified in an Irish HIBM patient (13). D378Y reduced UDP-GlcNAc 2-epimerase activity, and A631V decreased ManNAc kinase activity. Together with clinical and pathological similarities, these biochemical and molecular genetic results suggest that DMRV and HIBM are actually the same disease.

Through our study, we obtained information about novel molecular aspects in GNE. The two catalytic domains of the GNE molecule do not always work separately or independently in contrast to a published report (13). For example, the A524V mutation is within the predicted ManNAc kinase domain; however, it strongly inhibited UDP-GlcNAc 2-epimerase. Interestingly, this mutant did not form an oligomeric structure similar to the other N-terminal mutants. The failure of oligomerization in this A524V mutant is probably responsible for the reduced UDP-GlcNAc 2-epimerase activity as suggested previously (13).

Sialylation was decreased in muscle and in cultured cells from patients but was not completely lost, because all of the mutant proteins with missense mutations partially retained both enzymatic activities. Sialic acid levels in sera from DMRV patients were normal. Sialic acids are predominantly produced in the liver and transferred to synthesized glycoproteins. The sialylated proteins are released into the blood plasma, and free sialic acid in the plasma is derived from desialylation of these glycoproteins. GNE is expressed in the liver in large amounts; therefore, the reduction in enzymatic activities by mutations may not significantly affect the synthesis of sialic acid in the livers of DMRV patients, and sialic acids are present at concentrations comparable with normal blood levels. In contrast, in DMRV skeletal muscles, the sialic acid contents are reduced. The reduced enzymatic activities along with weak expression of GNE protein are probably responsible for the more serious reduction in sialic acid synthesis in muscle tissue compared with plasma. Lectin staining showed abnormal staining only in some fibers, indicating that a restricted number of myofibers has glycosylation abnormalities. This selective involvement may be due to muscle uptake of sialic acid, which can compensate for the defect of sialic acid synthesis in most fibers and explains why patients are normal at birth and develop late onset myopathies.

By feeding DMRV myotubes and fibroblasts with NeuAc as well as ManNAc, sialic acid concentrations in the cells increased to normal levels. As reported previously (21), treatment with NeuAc resulted in more rapid and potent effects on the restoration of sialylation than treatment with ManNAc. This strongly suggests that pharmacological therapy may be effective against DMRV/HIBM. Interestingly, even in myotubes harboring mutations that severely decrease ManNAc kinase activity, sialylation was restored by treatment with ManNAc. Schwarzkopf *et al.* (10) also reported similar observations in the embryonic stem cell culture in which the *GNE* gene was disrupted. They suggested that another sugar kinase may convert ManNAc to ManNAc-6-phosphate in those cells; therefore, ManNAc kinase activity of GNE may not be essential for sialic acid synthesis. If so, then why do the *GNE* mutations retaining UDP-GlcNAc 2-epimerase activity cause loss of sialylation and disease? One possible explanation is that these mutations may destabilize the GNE molecule resulting in decreased amounts of mutated proteins. However, we did not detect any reductions in the expressed amounts or defects in oligomerization of ManNAc-mutated recombinant proteins. Further analysis is necessary to clarify the mechanisms for the rescue resulting from the addition of ManNAc.

Enhanced staining with SBA lectin was observed in the sarcolemma and within the cytoplasmic area of some myofibers. These fibers were clustered and tended to be atrophic or have rimmed vacuoles. There is a report describing negative staining with SBA in Duchenne and Becker muscular dystrophies (22), suggesting that it is probably not because of dystrophic changes of myofibers but rather because of the lack of sialic acids. This abnormal glycosylation apparently preceded the formation of rimmed vacuoles, which is a pathological hallmark of DMRV. These rimmed vacuoles were electron-microscopically recognized as focal accumulations of autophagic vacuoles, which sometimes surround degenerated myofibrils and amyloid deposits. However, it is unknown whether the focal accumulations of autophagic vacuoles are the cause or result of the degeneration of myofibrils and amyloid deposits. Hypo-sialylation and abnormal glycosylation could cause the misfolding of some glycoproteins, and thus these misfolded glycoproteins may be targets of autophagic degradation and also behave as cores for formation of amyloid deposits. In our study, dystroglycan and SSA lectin staining was variable among patients. One possible explanation is that sialylation may not be the direct cause of the disease. For example, the loss of GNE enzymatic activity may induce the accumulation of the substrate, UDP-GlcNAc, leading to the abnormal *O*-GlcNAc modification of various proteins in the cells (23). Nevertheless, this possibility may also be unlikely because the overexpression of *O*-GlcNAc transferase did not cause any morphological abnormality in skeletal muscles in mice (24). In the next step, further analyses using animal models, as well as further testing of therapy with ManNAc or NeuAc, will be necessary to clarify the pathomechanism of DMRV and HIBM and the pathway from hyposialylation to rimmed vacuole formation and muscle atrophy.

Acknowledgments—We thank Dr. M. Hirano (Columbia University) for reviewing the manuscript, C. Yoshioka (National Center of Neurology and Psychiatry) for technical assistance in drawing figures. The monoclonal antibody H4A3, developed by Drs. J. T. August and J. E. K. Hildreth, was obtained from the Developmental Studies Hybridoma Bank developed under the auspices of the NICHD, National Institutes of Health, and maintained by The University of Iowa, Department of Biological Sciences, Iowa City, IA.

REFERENCES

1. Nonaka, I., Sunohara, N., Ishiura, S., and Satoyoshi, E. (1981) *J. Neurol. Sci.* **51,** 141–155
2. Nonaka, I., Murakami, N., Suzuki, Y., and Kawai, M. (1998) *Neuromuscul. Disord.* **8,** 333–337
3. Nonaka, I., Sunohara, N., Satoyoshi, E., Terasawa, K., and Yonemoto, K. (1985) *Ann. Neurol.* **17,** 51–59
4. Griggs, R. C., Askanas, V., DiMauro, S., Engel, A., Karpati, G., Mendell, J. R., and Rowland, L. P. (1995) *Ann. Neurol.* **38,** 705–713
5. Eisenberg, I., Avidan, N., Potikha, T., Hochner, H., Chen, M., Olender, T., Barash, M., Shemesh, M., Sadeh, M., Grabov-Nardini, G., Shmilevich, I., Friedmann, A., Karpati, G., Bradley, W. G., Baumbach, L., Lancet, D., Asher, E. B., Beckmann, J. S., Argov, Z., and Mitrani-Rosenbaum, S. (2001) *Nat. Genet.* **29,** 83–87
6. Ikeuchi, T., Asaka, T., Saito, M., Tanaka, H., Higuchi, S., Tanaka, K., Saida, K., Uyama, E., Mizusawa, H., Fukuhara, N., Nonaka, I., Takamori, M., and Tsuji, S. (1997) *Ann. Neurol.* **41,** 432–437
7. Eisenberg, I., Thiel, C., Levi, T., Tiram, E., Argov, Z., Sadeh, M., Jackson, C. L., Thierfelder, L., and Mitrani-Rosenbaum, S. (1999) *Genomics* **55,** 43–48
8. Nishino, I., Noguchi, S., Murayama, K., Driss, A., Sugie, K., Oya, Y., Nagata, T., Chida, K., Takahashi, T., Takusa, Y. Ohi, T., Nishimiya, J., Sunohara, N., Ciafaloni, E., Kawai, M., Aoki, M., and Nonaka, I. (2002) *Neurology* **59,** 1689–1693
9. Hinderlich, S., Stasche, R., Zeitler, R., and Reutter, W. (1997) *J. Biol. Chem.* **272,** 24313–24318
10. Schwarzkopf, M., Knobeloch, K. P., *Rohde, E., Hinderlich,* S., Wiechens, N., Lucka, L., Horak, I., Reutter, W., and Horstkorte, R. (2002) *Proc. Natl. Acad. Sci. U. S. A.* **99,** 5267–5270
11. Eisenberg, I., Grabov-Nardini, G., Hochner, H., Korner, M., Sadeh, M., Bertorini, T., Bushby, K., Castellan, C., Felice, K., Mendell, J. Merlini, L., Shilling, C., Wirguin, I., Argov, Z., and Mitrani-Rosenbaum, S. (2003) *Hum. Mutat.* **21,** 99
12. Lucka, L., Krause, M., Danker, K., Reutter, W., and Horstkorte R. (1999) *FEBS Lett.* **454,** 341–344
13. Effertz, K., Hinderlich, S., and Reutter, W. (1999) *J. Biol. Chem.* **274,** 28771–28778
14. Michele, D. E., Barresi, R., Kanagawa, M., Saito, F., Cohn, R. D., Satz, J. S., Dollar, J., Nishino, I., Kelley, R. I., Somer, H., Straub, V., Mathews, K. D., Moore, S. A., and Campbell, K. P. (2002) *Nature* **418,** 417–422
15. Noguchi, S., Wakabayashi, E., Imamura, M., Yoshida, M., and Ozawa, E. (2000) *Eur. J. Biochem.* **267,** 640–648
16. Shibuya, N., Tazaki, K., Song, Z. W., Tarr, G. E., Goldstein, I. J., and Peumans, W. J. (1989) *J. Biochem. (Tokyo)* **106,** 1098–1103
17. Yamamoto, K., Konami, Y., and Irimura, T. (1997) *J. Biochem. (Tokyo)* **121,** 756–761
18. Pereira, M. E., Kabat, E. A., and Sharon, N. (1974) *Carbohydr. Res.* **37,** 89–102
19. Keppler, O. T., Hinderlich, S., Langner, J., Schwartz-Albiez, R., Reutter, W., and Pawlita, M. (1999) *Science* **284,** 1372–1376
20. Bhavanandan, V. P., and Katlic, A. W. (1979) *J. Biol. Chem.* **254,** 4000–4008
21. Oetke, C., Hinderlich, S., Brossmer, R., Reutter, W., Pawlita, M., and Keppler, O. T. (2001) *Eur. J. Biochem.* **268,** 4553–4561
22. Paljarvi, L., Karjalainen, K., and Kalimo, H. (1984) *Arch. Neurol.* **41,** 39–42
23. Comer, F. I., and Hart, G. W. (2000) *J. Biol. Chem.* **275,** 29179–29182
24. McClain, D. A., Lubas, W. A., Cooksey, R. C., Hazel, M., Parker, G. J., Love, D. C., and Hanover, J. A. (2002) *Proc. Natl. Acad. Sci. U. S. A.* **99,** 10695–10699

ELSEVIER

Journal of the Neurological Sciences 219 (2004) 89–93

Journal of the Neurological Sciences

www.elsevier.com/locate/jns

FSHD-like patients without 4q35 deletion

Gaku Yamanaka[a,b], Kanako Goto[a], Tadayuki Ishihara[c], Yasushi Oya[d], Tasuku Miyajima[b], Akinori Hoshika[b], Ichizo Nishino[a], Yukiko K. Hayashi[a,*]

[a] *Department of Neuromuscular Research, National Institute of Neuroscience, National Center of Neurology and Psychiatry (NCNP), 4-1-1 Ogawa-higashi, Kodaira, Tokyo 187-8502, Japan*

[b] *Department of Pediatrics, Tokyo Medical University, 6-7-1 Nishi-shinjuku, Sinjuku, Tokyo 160-0023, Japan*

[c] *Department of Neurology, National Hakone Hospital, 412 Kazamatsuri, Odawara, Kanagawa 250-0032, Japan*

[d] *Department of Neurology, National Center Hospital for Mental, Nervous and Muscular Disorders, NCNP 4-1-1 Ogawa-higashi, Kodaira, Tokyo, 187-8551, Japan*

Received 27 June 2003; received in revised form 10 October 2003; accepted 19 December 2003

Abstract

Facioscapulohumeral muscular dystrophy (FSHD) is characterized by progressive weakness and wasting of facial, shoulder-girdle and upper arm muscles. Despite of the characteristic clinical features, the diagnosis of FSHD is sometimes difficult because clinical symptoms are extremely variable including facial sparing type, limb-girdle type, and distal myopathy type. Most of the FSHD patients have a deletion in the subtelomeric region of chromosome 4q35 (FSHMD1A), however the linkage analysis in some families suggested genetic heterogeneity. In the present study, we identified 40 patients without a deletion in the 4q35 region (non-4q35del) among 200 Japanese patients who were clinically suspected to have FHSD. All non-4q35del patients had shoulder-girdle weakness and 75% also had facial weakness. Eight patients showed clinical features that were indistinguishable from FSHD, but two of them had Becker muscular dystrophy. FSHD is clinically, and most likely genetically, as well, variable. Other forms of muscular dystrophy can also mimic FSHD.

© 2004 Published by Elsevier B.V.

Keywords: Facioscapulohumeral muscular dystrophy (FSHD); Southern blotting; Chromosome 4q35; *Eco*RI fragment; Deletion; Becker muscular dystrophy

1. Introduction

Autosomal dominant facioscapulohumeral muscular dystrophy (FSHD) is the third most common form of muscular dystrophy. The gene locus has been mapped to the subtelomeric region of chromosome 4q35 and most patients show a deletion of this region (FSHMD1A; MIM 158900), although the responsible gene for FSHD has not yet been identified. Southern blotting analysis using probe p13E-11 reveals a short *Eco*RI fragment in the 4q35 region, which contains the 3.3-kb *Kpn*I repeats (D4Z4) [1–8]. The homologous tandem repeats of 3.3-kb *Kpn*I units are also present on chromosome 10q26 and crosshybridized by p13E-11. However, a *Bln*I restriction enzyme site within each repeat from 10q26 allows differentiation of the two loci without haplotype analysis [9].

Clinical features of FSHD are characterized by progressive weakness and wasting of facial, shoulder-girdle and upper arm muscles. Most patients subsequently show involvement of peroneal and pelvic girdle muscles as well, and eventually 20% of the patients are wheelchair bound by the age of 40 years [10,11]. Nevertheless, clinical diagnosis of FSHD is sometimes difficult, because the phenotypic expression, even within the same family, is extremely variable, ranging from severe disability to being almost asymptomatic [12]. Facial muscles are spared in some patients, and others may show limb-girdle or distal dominant muscle involvement.

During genetic analysis of the FSHD patients, we found a certain number of patients who did not have a short *Eco*RI fragment on chromosome 4q35 although they had a clinical diagnosis of FHSD. In the present study, we focused on these patients and compared their clinicopathological find-

* Corresponding author. Tel.: +81-423-41-2711; fax: +81-423-46-1742.
E-mail address: hayashi_y@ncnp.go.jp (Y.K. Hayashi).

0022-510X/$ - see front matter © 2004 Published by Elsevier B.V.
doi:10.1016/j.jns.2003.12.010

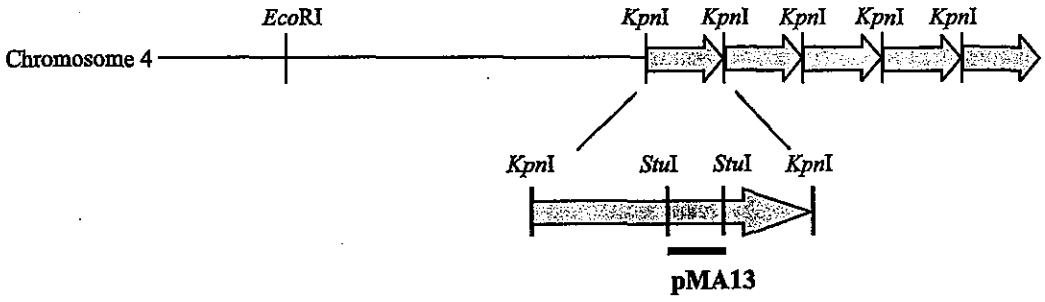

Fig. 1. The location of the probe pMA13. pMA13 is a 1.3kb *Stu*I fragment within each repeated *Kpn*I unit (D4Z4) on chromosome 4q35.

ings with those of patients with genetically confirmed FSHMD1A.

2. Materials and methods

2.1. Clinical materials

We studied 200 unrelated Japanese patients clinically suspected to have FSHD on examination by at least one neurologist. Since the clinical features of FSHD is quite variable, we labeled the patients as 'typical-FSHD-type' in the present study when all of the following four clinical criteria were satisfied: (1) weakness initially in facial or shoulder-girdle muscles, (2) progressive weakness or wasting of facial and shoulder-girdle muscles, (3) sparing of extra-ocular, masticatory, pharyngeal, lingual and cardiac muscles, (4) absence of severe or diffuse joint contractures.

Ninety-six unrelated healthy individuals of age over 60 years were also examined as control, since these older individuals had low risk to become symptomatic FSHD patients.

2.2. Genetic analysis

We obtained informed consent from all the patients and controls. Genomic DNA was isolated from peripheral blood lymphocytes using standard methods. To distinguish between the *Eco*RI fragments from 4q35 (*Bln*I-resistant) and from 10q26 (*Bln*I-sensitive), the DNA was digested with *Eco*RI and *Eco*RI/*Bln*I for conventional analysis and *Eco*RI/*Hin*dIII and *Eco*RI/*Bln*I for pulsed field gel electrophoresis (PFGE). After separation by both conventional gel electrophoresis and PFGE, we performed Southern blot analysis using two probes of p13E-11 and pMA13. The probe pMA13 is a 1.3 kb *Stu*I fragment within each repeated *Kpn*I unit (Fig. 1), which can identify patients with a deletion in the region of probe p13E-11, and also detect the exact size of the *Eco*RI fragment in patients with hybrid repeats of 4q35 and 10q26.

We also performed multiplex PCR analysis for the dystrophin gene, as previously described [13,14].

2.3. Histopathological analysis of muscle biopsies

Muscle biopsies from nine patients with 'non-4q35del' were frozen in liquid nitrogen-cooled isopentane. Serial frozen sections were stained with a battery of histochemical methods and immunostained with the following monoclonal antibodies: anti-dystrophin (NCL-DYS1, DYS2 and DYS3, Novocastra Laboratories, Newcastle upon Tyne, UK), anti-α-sarcoglycan (LNC-a-SARC, Novocastra Laboratories), anti-α-dystroglycan (VIA4-1, Upstate Biotechnology, Lake Placid, NY, USA), anti-β-dystroglycan (43 DAG1/8D5, Novocastra Laboratories), anti-laminin α2 chain (5 H2, Chemicon International, CA, USA), anti-caveolin-3 (BD Transduction Laboratories, KY, USA) and anti-dysferlin (NCL-Hamlet2, Novocastra Laboratories).

3. Results

We analyzed 96 healthy individuals over 60 years old by Southern blot analysis using the probe p13E-11, as control.

Table 1
Comparison of clinical features of FSHMD1A and non-4q35del patients

	Weakness				Regression of symptoms[a]	Sever joint contracture[a]	Initial symptom				High CK[b]
	Facial	*Shoulder-girdle*	*limb-girdle*	e, m, p, t[a]			Facial	Shoulder-girdle	Facial and shoulder-girdle	Limb-girdle[a]	
FSHMD1A	96.0	100	86.0	12.5	0	0	35.6	49.3	9.4	5.6	5.0
Non-4q35del	75.0	100	90.0	35.0	2.5	0	12.5	47.5	0	22.5	1.3

e, extra-ocular; m, masticatory; p, pharyngeal; t, tongue.
[a] Exclusion criteria of FSHD.
[b] Serum CK level over 1000 IU\log.

Table 2
Clinical features of eight non-4q35del patients showing typical-FSHD-type

Patient no.	SP/F	Age/sex (year)	Onset (year)	Initial symptom	Muscle weakness			Asymmetry	Progression	CK (IU/l)	*Eco*RI (kb)	Other clinical features
					f	s	l					
1	SP	24/M	8	s	+	+	+	+	+	ND	38	arrhythmia
2	SP	24/M	10	f	+	+	+	+	+	665	40	
3	F	20/M	7	s	+	+	+	+	+	738	48	RD
4	SP	13/M	11	s	+	+	+	–	+	69	>50	HL
5	F	25/M	15	s	+	+	ND	+	+	956	>50	
6	SP	63/F	40	s	+	+	+	+	+	455	>50	HL, RD
7[a]	SP	35/M	5	s	+	+	+	–	+	1266	36	
8[a]	F	29/M	7	f	+	+	+	+	+	ND	>50	

SP/F, sporadic/familial; M, male; F, female.
f, facial muscle (orbicularis oculi, peri-oral muscles); s, shoulder-girdle muscle; l, limb-girdle muscle.
*Eco*RI, *Eco*RI fragment size from 4q35; ND, not described.
HL, hearing loss; RD, respiratory disturbance.
[a] BMD.

We found five individuals who had a *Eco*RI digested fragment from 4q35 less than 40 kb; one had a 35 kb, one had a 36 kb, and three individuals had a 38 kb fragment. From this result, we designated our patients who had a short *Bln*I-resistant *Eco*RI fragment less than 35 kb on chromosome 4q35 as 'FSHMD1A', and the remaining were as 'non-4q35del', in the present study.

Among 200 patients clinically suspected to have FSHD, 160 patients had a short *Eco*RI fragment (<35 kb) on chromosome 4q35 and FSHMD1A was the diagnosis. The fragment size varied from 10 to 27 kb. The clinical features of the 160 patients are summarized in Table 1. In these patients, 126 (79%) showed all the typical-FSHD-type features, while 34 patients showed only some of the four criteria of typical-FSHD. Interestingly, 29 patients (18%) had symptoms usually considered to be exclusion criteria of FSHD [15]: extra-ocular (one patient), masticatory (four patients), pharyngeal (seven patients), lingual (13 patients) and onset in limb-girdle muscles (nine patients), which indicated that these exclusion criteria are not always reliable for ruling out the diagnosis of FSHD. No FSHMD1A patient showed regression of symptoms, severe joint contractures or cardiomyopathy.

By both of conventional and pulsed-field gel electrophoresis, 40 among 200 unrelated patients (20%) did not have a short *Eco*RI fragment from 4q35 of less than 35 kb, although they were clinically suspected to have FSHD (non-4q35del). The other probe pMA13 detected the same size fragments in all patients. The mean age at onset of the 40 non-4q35del patients was 19.2 years. Eight patients had family members with similar clinical symptoms. All patients showed shoulder-girdle muscle weakness. Ten patients (25%) did not have facial weakness (Table 1). Four patients had hearing loss, but none of the patients had retinal vasculopathy. Asymptomatic arrhythmia (five patients), mild respiratory disorders (11 patients), swallowing disturbances (four patients) were also found. The creatine kinase (CK) levels varied from 8 to 11,118 (normal ≦ 152 IU/l). There were myopathic changes in 94% and myopathic changes with scattered small angular fibers in 6% of the muscle biopsies. Nine muscle specimens were examined immunohistochemically, and showed no abnormality for all

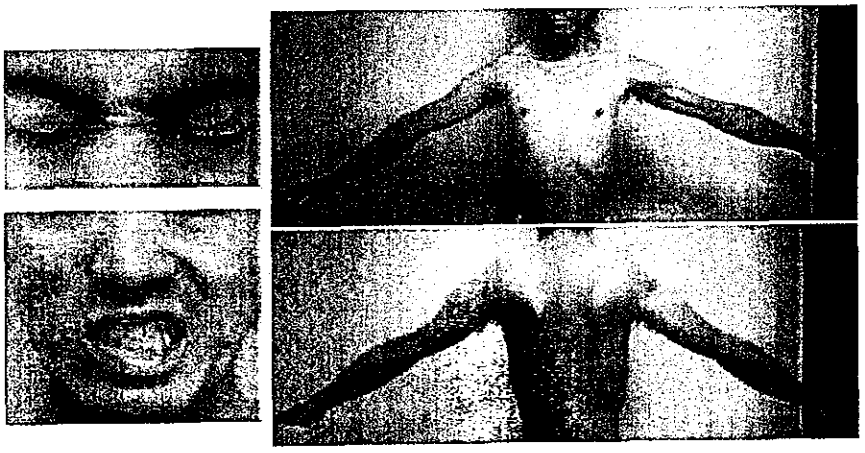

Fig. 2. A 24-year-old patient with typical-FSHD-type clinical features without a short *Eco*RI fragment (Pt.2 in Table 2). He first noted an asymmetrical smile and difficulties in lifting his arm with scapular winging at 10 years of age. Five years later, limb-girdle muscles were also involved.

the antibodies we used, except for one which showed a deficiency of caveolin-3. Electromyography (EMG) showed myopathic changes in 81% and mixed changes in 11%.

Eight patients in the non-4q35del group showed clinical features seen in the typical-FSHD patients, even though they had no short *Eco*RI fragment (Table 2). The age of onset was under 20 years except for one patient (Pt. 6) who became symptomatic at age 40 years. In all eight patients, facial muscles were involved and weakness of the shoulder and upper limb muscles was progressive (Fig. 2). The initial symptom in two patients was facial muscle involvement, while the other six patients first noted shoulder-girdle muscle weakness. Serum CK levels were mildly elevated in all except one patient (Pt. 4) whose level was within the normal range. To our great surprise, two of eight patients were found to have BMD by multiplex PCR analysis for the dystrophin gene (Fig. 3).

The remaining 32 patients without a short *Eco*RI fragment did not satisfy all of the four clinical criteria of typical FSHD. All had weakness of the shoulder-girdle muscles, but facial muscle involvement was present in 65%. There also were involvement of extraocular (nine patients), masticatory (four patients), lingual (three patients) and pharyngeal (three patients) muscles. By protein and gene analyses or electrophysiological analysis, we found that one patient had Emery-Dreifuss muscular dystrophy (AD-EDMD), another had limb-girdle muscular dystrophy type 1C (LGMD1C) and the third myasthenia gravis (MG).

Although shoulder-girdle muscles were involved in all 200 patients examined, facial muscle weakness was less common in non-4q35del group (75%) compared with FSHMD1A (96%). Although patients in both FSHMD1A and non-4q35del groups had exclusion criteria symptoms, they were more common in patients with non-4q35del (18 patients; 45%) than in FSHMD1A (29 patients; 18%). There was no marked difference in the histopathological and electrophysiological findings, except for one FSHMD1A patient who showed no abnormality on these examinations.

4. Discussion

Typical clinical symptoms of FSHD are characterized by a unique pattern of muscle involvement, which usually progresses in a descending manner, including weakness and atrophy of facial muscles, followed by shoulder-girdle, the scapula fixators, and the upper arm muscles. The clinical diagnosis, however, is sometimes difficult because of the extremely variable clinical features from the early onset severe form to clinically asymptomatic individuals. Several unusual clinical presentations have been reported including facial sparing type, limb-girdle type, and distal myopathy in genetically confirmed cases of FSHMD1A [16,17]. In the present study, 3.7% of genetically confirmed FSHMD1A patients showed facial sparing, and 18% presented with symptoms of the so-called exclusion criteria of FSHD [15], confirming the clinical variability of FSHMD1A.

On the other hand, 8 of 200 (4%) patients showed clinically typical-FSHD-type, although they had no deletion in the FSHD gene region. Interestingly, two of them turned out to have BMD by genetic analysis. The initial symptom was weakness of facial or shoulder-girdle muscles, but not limb-girdle muscles. Calf hypertrophy and cardiac involvement were not seen. One patient showed elevation of serum CK level (1266 IU/l). It should be noted that BMD patients can show clinical features indistinguishable from FSHD.

The remaining six clinically typical-FSHD patients without a short *Eco*RI fragment showed no abnormality by immunohistochemical and genetic analyses. It has been reported that approximately 5% of FSHD families fail to

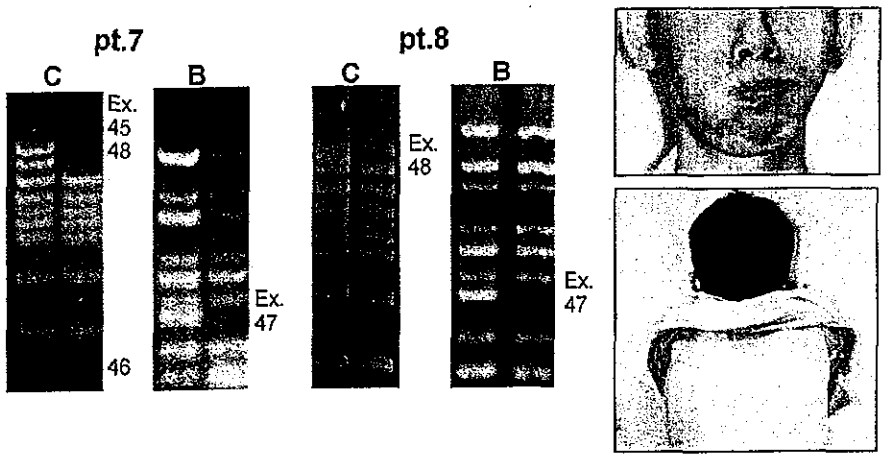

Fig. 3. Multiplex PCR analysis for the dystrophin gene of two typical-FSHD-type patients without a short *Eco*RI fragment. Pt.7 had a deletion from exons 45 to 48, and Pt.8 showed a deletion of exons 47 and 48. Asymmetrical facial muscle involvement and also atrophy of shoulder-girdle muscles were observed in Pt. 8. Two primer sets by Chamberlain (C) and Beggs (B) were used [13,14].

exhibit linkage to 4q35 [18]. These results suggest the genetic heterogeneity of this disease.

Since the responsible gene for FSHD has not been identified, genetic diagnosis is based on Southern blot analysis. The size of the *Eco*RI fragment is a critical determinant of clinical severity. Patients with the smallest size (10–11 kb) showed severe and wide varieties of clinical features [19–21]. On the other hand, several families were recently reported to have typical clinical features of FSHD with a *Eco*RI fragments greater than 35 kb [22,23]. These findings may expand the range of the *Eco*RI fragment size diagnostic of FSHD, but recent report showed the difficulty to define the molecular diagnostic cut-off point between FSHMD1A patients and the control population [24]. In the present study, we found five healthy individuals with a short *Eco*RI fragment of less than 40 kb. On the other hand, five non-4q35del patients had *Eco*RI fragment between 35 and 40 kb, and three of them showed typical-FSHD phenotypes, including BMD patient with 36 kb (Pt.1, 2 and 7 in Table 2). However, we did not label them as having FSHMD1A, since we could not perform linkage analysis because of the small size of the families. The role of the shortened D4Z4 repeats should be clarified to understand the pathomechanism of this complicated disease.

Acknowledgements

We thank Dr. S.M. Sumi, University of Washington, for his helpful discussion and advice. This work was supported by the Research Grants-in-Aid for Nervous and Mental Disorders, Research on Psychiatric and Neurological Diseases from the Ministry of Health, Labour and Welfare, and Grant-in-Aid for Scientific Research (C) from the Ministry of Education, Culture, Sports, Science and Technology, Japan.

References

[1] Wijmenga C, Frants RR, Brouwer OF, Moerer P, Weber JL, Padberg GW. Location of facioscapulohumeral muscular dystrophy gene on chromosome 4. Lancet 1990;336:651–3.
[2] Wijmenga C, Padberg GW, Moerer P, et al. Mapping of facioscapulohumeral muscular dystrophy gene to chromosome 4q35-qter by multipoint linkage analysis and in situ hybridization. Genomics 1991;9:570–5.
[3] Wijmenga C, Hewitt JE, Sandkuijl LA, et al. Chromosome 4q DNA rearrangements associated with facioscapulohumeral muscular dystrophy. Nat Genet 1992;2:26–30.
[4] van Deutekom JC, Wijmenga C, van Tienhoven EA, et al. FSHD associated DNA rearrangements are due to deletions of integral copies of a 3.2 kb tandemly repeated unit. Hum Mol Genet 1993;2:2037–42.
[5] Hewitt JE, Lyle R, Clark LN, et al. Analysis of the tandem repeat locus D4Z4 associated with facioscapulohumeral muscular dystrophy. Hum Mol Genet 1994;3:1287–95.
[6] Winokur ST, Bengtsson U, Feddersen J, et al. The DNA rearrangement associated with facioscapulohumeral muscular dystrophy involves a heterochromatin-associated repetitive element: implications for a role of chromatin structure in the pathogenesis of the disease. Chromosom Res 1994;2:225–34.
[7] Lee JH, Goto K, Matsuda C, Arahata K. Characterization of a tandemly repeated 3.3-kb *Kpn*I unit in the facioscapulohumeral muscular dystrophy (FSHD) gene region on chromosome 4q35. Muscle Nerve 1995:S6–S13.
[8] Goto K, Lee JH, Matsuda C, Hirabayashi K, et al. DNA rearrangements in Japanese facioscapulohumeral muscular dystrophy patients: clinical correlations. Neuromuscul Disord 1995;5:201–8.
[9] Deidda G, Cacurri S, Piazzo N, Felicetti L. Direct detection of 4q35 rearrangements implicated in facioscapulohumeral muscular dystrophy (FSHD). J Med Genet 1996;33:361–5.
[10] Padberg GW. Facioscapulohumeral disease. MD Thesis. Leiden: University of Leiden; 1982.
[11] Padberg GW, Lunt PW, Koch M, Fardeau M. Facioscapulohumeral muscular dystrophy. In: Emery AE, editor. Diagnostic criteria for neuromuscular disorders. 2nd ed. The Netherlands: European Neuromuscular Center; 1997. p. 9–15.
[12] Tawil R, Figlewicz DA, Griggs RC, Weiffenbach B. Facioscapulohumeral dystrophy: a distinct regional myopathy with a novel molecular pathogenesis. FSH Consortium. Ann Neurol 1998;43: 279–82.
[13] Beggs AH, Koenig M, Boyce FM, Kunkel LM. Detection of 98% of DMD/BMD gene deletions by polymerase chain reaction. Hum Genet 1990;86:45–8.
[14] Beggs AH. Multiplex PCR for identifying dystrophin gene deletions. In: Dracopoli NC, Haines JL, Korf BR, et al, editors. Current protocols in human genetics. New York: Greene and John Wiley and Sons; 1994. p. 9.3.1–17.
[15] Padberg GW, Lunt PQ, Koch M, Fardeau M. Facioscapulohumeral muscular dystrophy. In: AEHE, editor. Diagnostic criteria for neuromuscular disorders. The Netherlands: European Neuromuscular Center; 1994. p. 19–24.
[16] Felice KJ, Moore SA. Unusual clinical presentations in patients harboring the facioscapulohumeral dystrophy 4q35 deletion. Muscle Nerve 2001;24:352–6.
[17] Felice KJ, North WA, Moore SA, Mathews KD. FSH dystrophy 4q35 deletion in patients presenting with facial-sparing scapular myopathy. Neurology 2000;23:1927–31.
[18] Gilbert JR, Stajich JM, Wall S, et al. Evidence for heterogeneity in facioscapulohumeral muscular dystrophy (FSHD). Am J Hum Genet 1993;53:401–8.
[19] Yamanaka G, Goto K, Matsumura T, et al. Tongue atrophy in facioscapulohumeral muscular dystrophy. Neurology 2001;57:733–5.
[20] Yamanaka G, Goto K, Hayashi YK, et al. Clinical and genetical features of Japanese early-onset facioscapulohumeral muscular dystrophy. No To Hattatsu 2002;34:318–24.
[21] Funakoshi M, Goto K, Arahata K. Epilepsy and mental retardation in a subset of early onset 4q35-facioscapulohumeral muscular dystrophy. Neurology 1998;50:1791–4.
[22] Busse K, Kohler J, Stegmann K, et al. An inherited 4q35-EcoRI-DNA-fragment of 35 kb in a family with a sporadic case of facioscapulohumeral muscular dystrophy (FSHD). Neuromuscul Disord 2000;10:178–81.
[23] Vitelli F, Villanova M, Malandrini A, et al. A. Inheritance of a 38-kb fragment in apparently sporadic facioscapulohumeral muscular dystrophy. Muscle Nerve 1999;22:1437–41.
[24] Buts M, Koch MC, Muller-Felber W, et al. Facioscapulohumeral muscular dystrophy Phenotype–genotype correlation in patients with borderline D4Z4 repeat numbers. J Neurol 2003;250:932–7.

J. Biochem. 135, 709–712 (2004)
DOI: 10.1093/jb/mvh086

Subcellular Localization of Fukutin and Fukutin-Related Protein in Muscle Cells

Hiroshi Matsumoto[1,2], Satoru Noguchi[1,3,*], Kazuma Sugie[1], Megumu Ogawa[1,3], Kumiko Murayama[1], Yukiko K. Hayashi[1] and Ichizo Nishino[1,3]

[1]Department of Neuromuscular Research, National Institute of Neuroscience, National Center of Neurology and Psychiatry (NCNP), Tokyo 187-8502; [2]Department of Pediatrics, National Defense Medical College, Saitama, 359-8513; [3]Core Research for Evolutional Science and Technology (CREST), Japan Science and Technology Corporation, Saitama 332-0012

Received March 29, 2004; accepted April 13, 2004

Fukuyama-type congenital muscular dystrophy and congenital muscular dystrophy 1C are congenital muscular dystrophies that commonly display reduced levels of glycosylation of α-dystroglycan in skeletal muscle. The genes responsible for these disorders are *fukutin* and *fukutin-related protein* (*FKRP*), respectively. Both gene products are thought to be glycosyltransferases, but their functions have not been established. In this study, we determined their subcellular localizations in cultured skeletal myocytes. FKRP localizes in rough endoplasmic reticulum, while fukutin localizes in the *cis*-Golgi compartment. FKRP was also localized in rough endoplasmic reticulum in skeletal muscle biopsy sample. Our data suggest that fukutin and FKRP may be involved at different steps in *O*-mannosylglycan synthesis of α-dystroglycan, and FKRP is most likely involved in the initial step in this synthesis.

Key words: *cis*-Golgi, fukutin, fukutin-related protein, rough, endoplasmic reticulum, skeletal muscle.

Abbreviations: DG, dystroglycan; ER, endoplasmic reticulum; FCMD, Fukuyama-type congenital muscular dystrophy; FKRP, fukutin-related protein; MDC1C, congenital muscular dystrophy 1C; POMT1, protein *O*-mannosyltransferase 1.

Congenital muscular dystrophy comprises a genetically heterogeneous group of disorders. Fukuyama-type congenital muscular dystrophy (FCMD), the most common congenital muscular dystrophy in Japan, is characterized by muscle weakness and hypotonia from early infancy, and is associated with mental retardation and a brain anomaly called type II lissencephaly. The causative gene was cloned in 1998 and named *fukutin*, and a 3-kb retrotransposal insertion in the 3′-untranslated region of *fukutin* is found in most patients with FCMD (*1*). Fukutin-related protein (FKRP) was characterized as a homolog of fukutin in 2001 (*2*), and mutations in *FKRP* were also shown to cause muscular dystrophies (congenital muscular dystrophy 1C (MDC1C) and limb-girdle muscular dystrophy 2I) (*2*, *3*).

Skeletal muscle biopsy samples from FCMD and MDC1C patients show a marked reduction in α-dystroglycan (α-DG) by immunostaining with an antibody against the glycosylated epitope (*2*, *5*), whereas α-DG could still be visualized even in FCMD skeletal muscle with an antibody that recognizes the peptide epitope (*6*). The reduction in α-DG glycosylation in skeletal muscle leads to a loss in its ability to bind to extracellular ligands such as laminin, agrin and neurexin (*6*). Thus, the abnormality in posttranslational glycosylation of α-DG plays a crucial role in the pathogenesis of FCMD and MDC1C. The functions of fukutin and FKRP have not been clarified. However, they are supposed to act as glycosyltransferases, because they both are type-II transmembranous proteins and possess a DXD motif in the C-terminal side that is often found in glycosyltransferases (*4*). These facts strongly indicate that these two proteins may participate in the glycosylation of α-DG.

Protein glycosylation is a highly organized orderly process. Newly synthesized naked proteins are sequentially modified *en route* by glycosyltransferases during transport from the rough endoplasmic reticulum (ER) to the *trans*-Golgi network (*7*). Therefore, the expression and localization of a glycosyltransferase must be precisely regulated to synthesize the specific glycostructure in each tissue and cell. Determining the localization of putative glycosyltransferases will help to predict their functions. In this study, we determined the precise localization of fukutin and FKRP in muscle cells.

MATERIALS AND METHODS

Antibodies—Anti-FKRP and anti-fukutin antibodies were raised in rabbits against the recombinant fragments comprising the carboxyl-terminal 112 and 121 amino acids, respectively. Expression vectors for the FKRP and fukutin fragments with a glutathione-*S*-transferase tag at the N-terminus were constructed by inserting the cDNA fragments into pGEX-4T (Amarsham). Both antibodies were affinity-purified on antigen-immobilized activated thiol-Sepharose 4B (Amersham Pharmacia Biotec). Other antibodies used in this study are anti-emerin (Novocastra Laboratories), anti-BiP, anti-calnexin, anti-

*To whom correspondence should be addressed. Tel: +81-423412712; Fax: +81-423461742 Email: noguchi@ncnp.go.jp

 © 2004 The Japanese Biochemical Society.

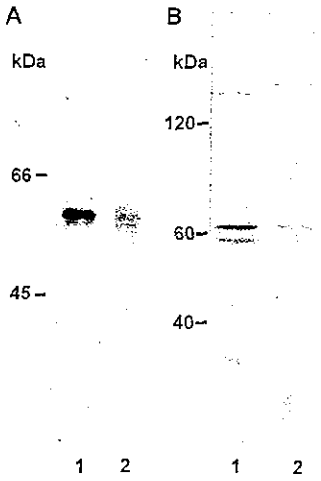

Fig. 1. **Characterization of newly raised polyclonal antibodies by Western blotting.** A: The anti-FKRP antibody detected a band at approximately 60 kDa in COS cell lysates with transiently expressed myc-FKRP (lane 1) and in human skeletal muscle cells (lane 2). B: Western blotting of a C2C12 cell lysate transfected with myc-fukutin. Both anti-fukutin (lane 1) and anti-myc (lane 2) antibodies detected doublet bands at approximately 60 kDa.

GM130 (BD Biosciences Pharmingen), and anti-myc 9E10 (Oncogene Science). Primary antibodies were used at the following dilutions: anti-FKRP (1:200), anti-fukutin (1:100), anti-myc (1:100), anti-BiP (1:100), anti-calnexin (1:100), anti-GM130 (1:500) and anti-emerin (1:500). Alexa 488-labeled anti-rabbit IgG and Alexa 568-labeled anti-mouse IgG (Molecular probes) were used as secondary antibodies.

cDNA Transfection and Immunocytochemistry—The open reading frames of FKRP and fukutin were amplified by PCR and subcloned into the expression vector CMV-myc (BD Clontech). These expression vectors encoding myc-epitope tagged FKRP and fukutin were transfected into the C2C12 cell line using Lipofectamine as described in the manufacturer's instructions (Invitrogen Carlsbad). The C2C12 cells and human skeletal muscle cells were induced to differentiate as described in a previous report (*8*). The immunostaining of myocytes was performed as described earlier (*9*). Laser confocal fluorescence images were obtained using an Olympus FLUOVIEW confocal microscope (Olympus).

Western Blotting and Immunohistostaining of Human Skeletal Muscles—Western blotting and immunohistostaining of human skeletal muscle were performed as described previously (*5*, *9*). The immunoreactive bands on Western blot were visualized using an ECL kit (Amersham Pharmacia Biotec). The immunostained sections were observed under a Zeiss Axiophot2 microscope (Carl Zeiss)

Muscle Biopsy Sample—Control muscle was obtained from surgical discards from a 24-yr-old male patient. Informed consent was obtained using the form approved by the Ethical Review Board at NCNP.

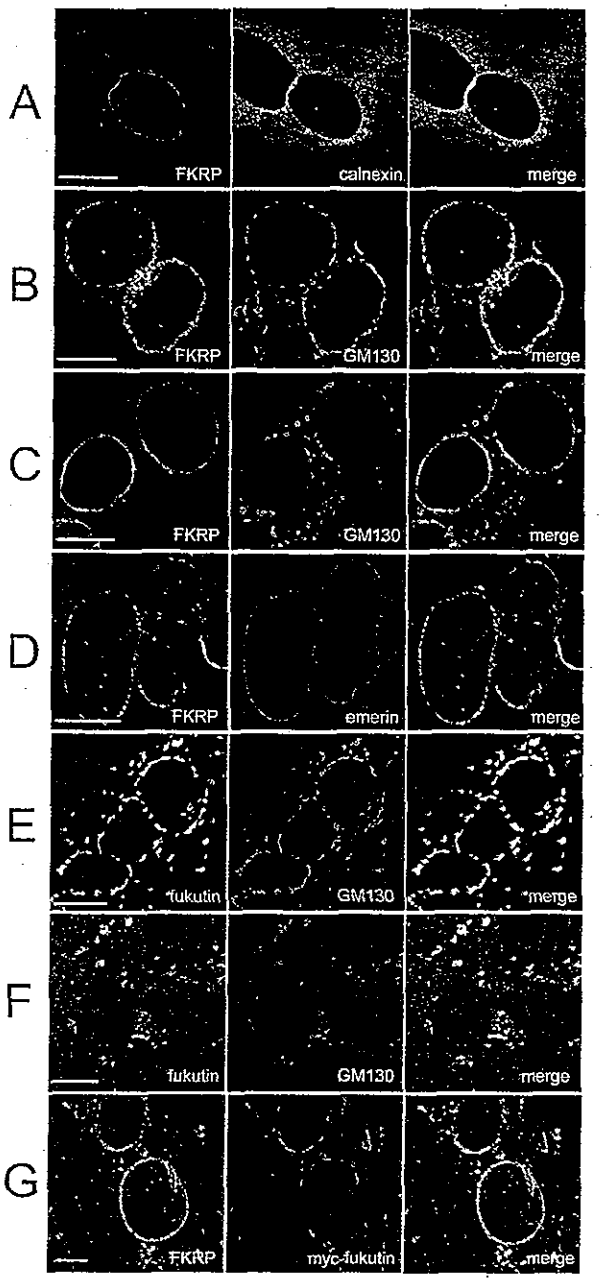

Fig. 2. **Subcellular localization of FKRP and fukutin.** A: FKRP and calnexin staining of human skeletal myotubes. FKRP (red) was continuously stained around nuclei with the innermost part of calnexin staining (green). B, C: FKRP and GM130 staining in mouse C2C12 myotubes. FKRP (green) was stained in the inner aspect of GM130 localization (red). Treatment with brefeldin A induced the dissociation of the Golgi apparatus, but FKRP remained localized around nuclei (C). D: FKRP and emerin staining in human skeletal myotubes. FKRP (green) was stained on the outer aspect of emerin staining (red). E, F: Immunostaining of transfected fukutin and GM130 in C2C12 myotubes. The merged image shows the co-localization of transfected fukutin and GM130. Treatment with brefeldin A dispersed both stainings into the cytosol (F). G: Spatial relationship between FKRP and fukutin. Endogenous FKRP (green) and transfected fukutin (red) in C2C12 myotubes showed different localizations. Bars denote 10 μm.

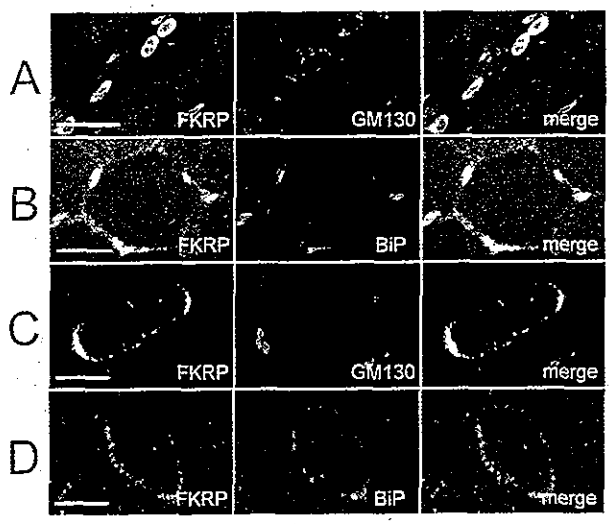

Fig. 3. **Immunohistochemical staining of FKRP in skeletal muscle.** The anti-FKRP antibody stained continuously around nuclei (A–D, green), while the anti-GM130 antibody stained nuclear poles and granular concentrates in cytosol (A, C, red). On higher magnifications, FKRP and GM130 are seen to overlap partially at both nuclear poles (C). BiP staining merges with FKRP in muscles (D). Bars denote 50 μm (A, B) and 5 μm (C, D).

RESULTS

Characterization of Newly Raised Antibodies against FKRP and Fukutin—Polyclonal antibodies against FKRP and fukutin were raised using recombinant fragments comprising the carboxyl-terminal 112 and 121 amino acids, respectively; the fragments share no homology to each other. Western blot analysis of a homogenate from cultured human skeletal muscle cells using the anti-FKRP antibody detected a band migrating at approximately 60 kDa (lane 2 in Fig. 1A), which matches the size of transiently expressed myc-FKRP in COS cells (lane 1).

The anti-fukutin antibody was not adequately sensitive to detect endogenous fukutin in skeletal muscle or in cultured muscle cell homogenates. In C2C12 muscle cells, in which myc-fukutin was transiently expressed, the anti-fukutin antibody detected two adjacent bands migrating at 60 kDa (lane 1 in Fig. 1B). The anti-myc antibody also detected two same sized bands (lane 2), suggesting that some posttranslational modification, such as glycosylation, generates the two bands. The specificity of each antibody was also examined by cross Western blot experiments in which the anti-FKRP antibody was allowed to react with the recombinant fukutin protein expressed in C2C12 cells, and the anti-fukutin antibody to react with the recombinant FKRP expressed in COS cells. No band was detected in either blotting, demonstrating the specificity of each antibody.

Subcellular Localization of FKRP and Fukutin in Differentiated Myocytes—To determine the subcellular localization of FKRP and fukutin in differentiated myocytes, human myocytes or C2C12 cells were immunostained with the two antibodies (Fig. 2). FKRP staining was detected surrounding the nuclei only in myotubes, but not in myoblasts. We compared this localization with those of organelle marker proteins against calnexin, a chaperone protein in rough ER (*10*). Calnexin localizes around the nuclei and merges with FKRP staining (Fig. 2A), although calnexin is also diffusely distributed in the cytosol. Double staining with antibodies for GM130, a matrix protein in the *cis*-Golgi compartment (*11*) or emerin, an inner nuclear membranous protein, showed that FKRP co-localizes with neither of them, the inner aspect of GM130 and outer aspect of emerin (Fig. 2B, D). After treating of the cells with brefeldin A, which induces the dissociation of the Golgi apparatus (*12*), GM130 staining was dispersed in the cytoplasm while FKRP staining was unaffected (Fig. 2C). These results suggest that FKRP is not localized in the Golgi or inner nuclear membrane but in the rough ER.

The staining of transfected C2C12 cells with antibodies against fukutin and its introduced tag showed the same distribution in the perinuclear area in a discontinuous dot-like pattern under confocal microscopy (data not shown). When transfected C2C12 cells were stained for fukutin and GM130, the two stains precisely overlapped (Fig. 2E), and treatment with brefeldin A dispersed both proteins (Fig. 2F). These phenomena indicate that fukutin is localized in the *cis*-Golgi in differentiated myocytes.

We compared the localization of FKRP and fukutin in C2C12 cells in which myc-fukutin was transiently expressed. FKRP and myc-fukutin displayed different localizations in myocytes (Fig. 2G).

Localization of FKRP in human skeletal muscle—In skeletal muscle biopsy specimens, FKRP was detected continuously around the nuclei of skeletal muscle fibers (Fig. 3A–D, green). After absorption of the FKRP antibody with recombinant FKRP protein, no staining was observed (data not shown). We compared this localization with those of organelle marker proteins against BiP, a chaperone protein in rough ER (*10*), and GM130. BiP was localized around the nuclei and merged with FKRP staining (Fig. 3B, D). GM130 was present at the poles of the nuclei and, in addition, a few concentrated granules were present within the cytosol and did not overlap with FKRP (Fig. 3A, C). These findings suggest that FKRP is localized in rough ER *in vivo*. Interestingly, in some nuclear poles, GM130 and FKRP staining was found to be partly merged (Fig. 3C). It is important to note that ER and the Golgi apparatus form an essentially continuous structure in the intracellular transport system, and that this is a possible explanation for the partial co-localization of FKRP and GM130.

DISCUSSION

The localization of FKRP is distinctly different from that of fukutin. Recently, Esapa et al. reported the subcellular localization of FKRP and fukutin in the medial-Golgi apparatus using rat kidney fibroblasts (*13*). Our data do not support the localization of FKRP in the Golgi apparatus, although immunohistochemical staining of skeletal muscle biopsy sample showed the partial incorporation of FKRP into other Golgi resident proteins. We assume that this difference is a result of the different cell types used in these two studies because FKRP colocalized with fukutin in CHO cells in which FKRP and myc-fukutin were transiently expressed (data not shown). In our experiments using C2C12 cells, endogenous FKRP was seen

only in differentiated myotubes, and the localization was different from those of GM130 and fukutin. Thus, we believe during muscle cell development, FKRP is expressed and functions in the rough ER after myotube formation. In addition, preliminary observations by immunoelectron microscopy demonstrated FKRP localization on the outer nuclear membrane or in transporting vesicles between the nuclear membrane and the Golgi apparatus, close to the distribution of ribosomes (unpublished data). It is unlikely that the localization of extrinsic fukutin is an artefact due to overexpression of this protein, because the extrinsic fukutin localizes only in the *cis*-Golgi apparatus in all transfected cells despite of its variable expression level.

Newly synthesized α-DG in the rough ER is thought to be modified by a series of glycosyltransferases, finally forming unique sugar chains consisting of *O*-mannosyl tetrasaccharide (Siaα2–3Galβ1–4GlcNAcβ1–2Man-*O*-protein) (*14*, *15*). The first *O*-mannosylation step is catalyzed by protein *O*-mannosyltransferase 1 (POMT1) (*16*), and this step may occur in rough ER. In fact, in yeast, several O-mannosyltransferases and their donor substrate, dolichyl-*P*-mannose, are indeed localized in rough ER (*17*). A mutation in *POMT1* causes Walker-Warburg syndrome, the most severe form of congenital muscular dystrophy with brain involvement, and it is also known that skeletal muscle biopsy samples from patients with Walker-Warburg syndrome show markedly reduced levels of α-DG (*16*, *18*). Our observations predict that FKRP localizes in rough ER, suggesting that FKRP may play a role in the first *O*-mannosylation step of α-DG with POMT1. Further analyses of the relationship between POMT1 and FKRP may clarify the role of FKRP in the *O*-mannosylation of α-DG.

In this study, we have clarified the precise subcellular localization of fukutin and FKRP in myocytes. The localization of both proteins suggests that they are involved in the glycosylation of α-DG, but in different manners. The biological characterization of fukutin and FKRP as glycosyltransferases and structural analyses of the α-DG sugar chains in patients are necessary to gain a complete understanding of the glycosylation process of α-DG, and, hence, the possible elucidation of the pathomechanism of FCMD and MDC1C.

This work was partly supported by the AYAKA Foundation.

REFERENCES

1. Kobayashi, K., Nakahori, Y., Miyake, M., Matsumura, K., Kondo-Iida, E., Nomura, Y., Segawa, M., Yoshioka, M., Saito, K., Osawa, M., Hamano, K., Sakakihara, Y., Nonaka, I., Nakagome, Y., Kanazawa, I., Nakamura, Y., Tokunaga, K., and Toda, T. (1998) An ancient retrotransposal insertion causes Fukuyama-type congenital muscular dystrophy. *Nature* **394**, 388–392
2. Brockington, M., Blake, D.J., Prandini, P., Brown, S.C., Torelli, S., Benson, M.A., Ponting, C.P., Estournet, B., Romero, N.B., Mercuri, E., Voit, T., Sewry, C.A., Guicheney, P., and Muntoni, F. (2001) Mutations in the fukutin-related protein gene (FKRP) cause a form of congenital muscular dystrophy with secondary laminin alpha2 deficiency and abnormal glycosylation of alpha-dystroglycan. *Amer. J. Hum. Genet.* **69**, 1198–1209
3. Brockington, M., Yuva, Y., Prandini, P., Brown, S.C., Torelli. S., Benson, M.A., Herrmann, R., Anderson, L.V., Bashir, R., Burgunder, J.M., Fallet, S., Romero, N., Fardeau, M., Straub, V., Storey, G., Pollitt, C., Richard, I., Sewry, C.A., Bushby, K., Voit, T., Blake, D.J., and Muntoni, F. (2001) Mutations in the fukutin-related protein gene (FKRP) identify limb girdle muscular dystrophy 2I as a milder allelic variant of congenital muscular dystrophy MDC1C. *Hum. Mol. Genet.* **10**, 2851–2859
4. Martin-Rendon, E., and Blake, D.J. (2003) Protein glycosylation in disease: new insights into the congenital muscular dystrophies. *Trends Pharmacol. Sci.* **24**, 178–183
5. Hayashi, Y.K., Ogawa, M., Tagawa, K., Noguchi, S., Ishihara, T., Nonaka, I., and Arahata, K. (2001) Selective deficiency of alpha-dystroglycan in Fukuyama-type congenital muscular dystrophy. *Neurology* **57**, 115–121
6. Michele, D.E., Barresi, R., Kanagawa, M., Saito, F., Cohn, R.D., Satz, J.S., Dollar, J., Nishino, I., Kelley, R.I., Somer, H., Straub, V., Mathews, K.D., Moore, S.A., and Campbell, K.P. (2002) Post-translational disruption of dystroglycan-ligand interactions in congenital muscular dystrophies. *Nature* **418**, 417–422
7. Alberts, B., Johnson A., Lewis, J., Raff, M., Roberts, K., and Walter, P. (2002) *Molecular Biology of the Cell* pp. 726–739, Garland Science, New York
8. Noguchi, S., Wakabayashi, E., Imamura, M., Yoshida, M., and Ozawa, E. (1999) Developmental expression of sarcoglycan gene products in cultured myocytes. *Biochem. Biophys. Res. Commun.* **262**, 88–93
9. Noguchi, S., Wakabayashi, E., Imamura, M., Yoshida, M., and Ozawa, E. (2000) Formation of sarcoglycan complex with differentiation in cultured myocytes. *Eur. J. Biochem.* **267**, 640–648
10. Kim, P.S., and Arvan, P. (1995) Calnexin and BiP act as sequential molecular chaperones during thyroglobulin folding in the endoplasmic reticulum. *J. Cell Biol.* **128**, 29–38.
11. Nakamura, N., Rabouille, C., Watson, R., Nilsson, T., Hui, N., Slusarewicz, P., Kreis, T.E., and Warren, G. (1995) Characterization of a cis-Golgi matrix protein, GM130. *J. Cell Biol.* **131**, 1715–1726
12. Fujiwara, T., Oda, K., Yokota, S., Takatsuki, A., and Ikehara, Y. (1988) Brefeldin A causes disassembly of the Golgi complex and accumulation of secretory proteins in the endoplasmic reticulum. *J. Biol. Chem.* **263**, 18545–18552
13. Esapa, C.T., Benson, M.A., Schroder, J.E., Martin-Rendon, E., Brockington, M., Brown, S.C., Muntoni, F., Kroger, S., and Blake, D.J. (2002) Functional requirements for fukutin-related protein in the Golgi apparatus. *Hum. Mol. Genet.* **11**, 3319–3331
14. Sasaki, T., Yamada, H., Matsumura, K., Shimizu, T., Kobata, A., and Endo, T. (1998) Detection of O-mannosyl glycans in rabbit skeletal muscle alpha-dystroglycan. *Biochim. Biophys. Acta* **1425**, 599–606
15. Chiba, A., Matsumura, K., Yamada, H., Inazu, T., Shimizu, T., Kusunoki, S., Kanazawa, I., Kobata, A., and Endo, T. (1997) Structures of sialylated O-linked oligosaccharides of bovine peripheral nerve alpha-dystroglycan. The role of a novel O-mannosyl-type oligosaccharide in the binding of alpha-dystroglycan with laminin. *J. Biol. Chem.* **272**, 2156–2162
16. Beltran-Valero de Bernabe, D., Currier, S., Steinbrecher, A., Celli, J., van Beusekom, E., van der Zwaag, B., Kayserili, H., Merlini, L., Chitayat, D., Dobyns, W.B., Cormand, B., Lehesjoki, A.E., Cruces, J., Voit, T., Walsh, C.A., van Bokhoven, H., and Brunner, H.G. (2002) Mutations in the O-mannosyltransferase gene POMT1 give rise to the severe neuronal migration disorder Walker-Warburg syndrome. *Amer. J. Hum. Genet.* **71**, 1033–1043
17. Strahl-Bolsinger, S., Gentzsch, M., and Tanner, W. (1999) Protein O-mannosylation. *Biochim. Biophys. Acta* **1426**, 297–307
18. Kim, D.S., Hayashi, Y.K., Matsumoto, H., Ogawa, M., Noguchi, S., Murakami, N., Sakuta, R., Mochizuki, M., Michele, D.E., Campbell, K.P., Nonaka, I., and Nishino, I. (2004) POMT1 mutation results in defective glycosylation and loss of laminin-binding activity in alpha-DG. *Neurology* **62**, 1009–1011

European Journal of Neurology 2004, 11: 657–661

Dysferlin mutation analysis in a group of Italian patients with limb-girdle muscular dystrophy and Miyoshi myopathy

K. Kawabe[a,b], K. Goto[a], I. Nishino[a], C. Angelini[c] and Y. K. Hayashi[a]

[a]*Department of Neuromuscular Research, National Institute of Neuroscience, National Center of Neurology and Psychiatry (NCNP), Tokyo, Japan;* [b]*The Fourth Department of Internal Medicine, Toho University School of Medicine, Tokyo, Japan;* [c]*Department of Neurological and Psychiatric Sciences, University of Padova, Padova, Italy*

Keywords:
dysferlin, limb-girdle muscular dystrophy (LGMD), Miyoshi myopathy (MM), mutation, polymorphism

Received 28 March 2003
Accepted 24 October 2003

Mutations in the dysferlin gene (*DYSF*) on chromosome 2p13 cause distinct phenotypes of muscular dystrophy: limb-girdle muscular dystrophy type 2B (LGMD2B), Miyoshi myopathy (MM), and distal anterior compartment myopathy, which are known by the term 'dysferlinopathy'. We performed mutation analyses of *DYSF* in 14 Italian patients from 10 unrelated families with a deficiency of dysferlin protein below 20% of the value in normal controls by immunoblotting analysis. We identified 11 different mutations, including eight missense and three deletion mutations. Nine of them were novel mutations. We also identified a unique 6-bp insertion polymorphism within the coding region of *DYSF* in 15% of Italian population, which was not observed in East Asian populations. The correlation between clinical phenotype and the gene mutations was unclear, which suggested the role of additional genetic and epigenetic factors in modifying clinical symptoms.

Introduction

Miyoshi myopathy (MM) is an early-adult onset, autosomal recessive form of distal muscular dystrophy, characterized by predominant involvement in the calf muscles and highly elevated serum creatine kinase (CK) levels (Miyoshi *et al.*, 1967, 1986). MM is caused by mutations in the dysferlin gene (*DYSF*) on chromosome 2p13 (Liu *et al.*, 1998a,b). Mutations in the same gene were also identified in patients with limb-girdle muscular dystrophy type 2B (LGMD2B) (Bashir *et al.*, 1998; Liu *et al.*, 1998a), and distal anterior compartment myopathy (Illa *et al.*, 2001). These diseases caused by mutations in *DYSF* are known by the term 'dysferlinopathy'. Dysferlin is a 237-kDa protein expressed predominantly in skeletal muscle which localizes to the plasma membrane of muscle fibers (Anderson *et al.*, 1999; Matsuda *et al.*, 1999). It is still unknown why mutations of the same gene cause either proximal LGMD or distal myopathies.

In the present study, we performed mutation analysis of *DYSF* in a group of families with a dysferlin protein deficiency, and found nine novel mutations and one unique insertion polymorphism in the coding region.

Correspondence: Yukiko K. Hayashi MD, Department of Neuromuscular Research, National Institute of Neuroscience, NCNP, 4-1-1 Ogawa-higashi, Kodaira, Tokyo, 187-8502 Japan (fax: +81 42 346 1742; e-mail: hayasi_y@ncnp.go.jp).

Methods

All clinical materials were obtained for diagnostic purposes with informed consent. We examined 14 Italian patients from 10 unrelated families who were clinically suspected of LGMD or MM, and showed a deficiency of dysferlin protein below 20% of the control value by immunoblotting analysis (Matsuda *et al.*, 1999; Fanin *et al.*, 2001). Genomic DNA and total RNA were isolated either from peripheral blood lymphocytes or biopsied skeletal muscles using a standard technique. Control genomic DNA samples were also obtained from 60 Italian, 50 Japanese, 50 Korean and 50 Chinese unrelated individuals.

For the haplotype analysis, we used three microsatellite markers: D2S292, D2S291, and D2S286 spanning *DYSF* on chromosome 2p, as described previously (Bejaoui *et al.*, 1995).

Specific primer sets for each 55 exon of *DYSF* were described previously (Liu *et al.*, 1998a). Polymerase chain reaction-single-strand conformational polymorphism (PCR-SSCP) was performed at three different temperatures: 5, 10 and 15°C, using a GenePhor DNA Separation System and a GeneGel Excel 12.5/24 Kit (Amersham Biosciences Co., Tokyo, Japan). To detect the deletion mutation from exons 25 to 29, reverse transcriptase-PCR (RT-PCR) was performed using following primer sets; Dysf6F: 5′-GGTGACATCCATGAGA CAAC-3′ (nt 2546–2565) and Dysf6R: 5′-GGACA-CACGAACCAATCTCC-3′ (nt 3155–3174), Dysf7F: 5′-GGAGATTGGTTCGTGTGTCC-3′ (nt 3155–3174)

© 2004 EFNS

and Dysf7R: 5′-CGATCTCGTAGAAGATGAGCG-3′ (nt 3979–3998), and Dysf6F and Dysf7R.

Direct sequencing of the PCR products was performed using a Long Read Tower (Amersham Biosciences). For the screening of control individuals, PCR-SSCP or PCR-restriction fragment length polymorphism (PCR-RFLP) was performed. For PCR-RFLP, we used *Hin*PI for exon 29, *Taq*I for exon 37, *Mae*III for exon 42, and *Ava*II for exon 44.

Results

The clinical summary of 14 patients from 10 unrelated families is shown in the Table 1. Different clinical phenotypes were observed within the same family in F2 and F6. From the results of PCR-SSCP and direct sequencing analyses, we identified 11 different mutations that included eight missense and three deletion mutations (Table 1). Nine of them were novel mutations. A total of 120 chromosomes from Italian control individuals were screened for all mutations by either PCR-SSCP or PCR-RFLP, and no control individual showed the same substitution or deletion that the affected patients had.

Patient 9 showed a possible homozygous large deletion of the gene which was the same one previously reported by Anderson *et al.* (2000) as a 'probable deletion'. Haplotype analysis using three microsatellite markers, D2S292, D2S291, and D2S286 on chromosome 2p, revealed that only the affected patients with the typical MM phenotype were homozygous in this region, while other unaffected family members were heterozygous (Fig. 1a). PCR amplification using genomic DNA showed no amplified products from exons 25 to 29, although the other exons were clearly amplified at the expected sizes (Fig. 1b). RT-PCR and direct sequencing analyses revealed two truncated transcripts with different sizes corresponding to the deletions from exons 25 to 29 and from exons 25 to 30 (Fig. 1c). Both of these altered transcripts were in-frame and produced truncated dysferlin proteins; however, immunoblotting analysis showed no detectable band in this patient (data not shown).

During the mutation screening, we found nine kinds of polymorphisms. They were 766C > T (P131P), 1315C > T (H314H), 2200T > C (D609D), 2446G > A (Q691Q), 2956T > C (S861S), 3438G > A (R1022Q), 3853G > A (Q1160Q), 4381C > A (I1336I), and one 6-bp insertion. The 3438G > A substitution resulted in an amino acid change in R1022Q, but this was observed in 21% of Italian control individuals. The 6-bp insertion of AGGCGG was located within the coding region (exon 30) of *DYSF*, causing a two amino acid (AE) insertion at amino acid number 1062 (Fig. 2a, b). Nine of 60 Italian control individuals (15%) had this 6-bp insertion heterozygously. This insertion was also observed in two families with dysferlinopathy. Patient 3 had this insertion heterozygously, and her healthy mother had it homozygously. All three patients in F6 also had this 6-bp insertion homozygously, together with a homozygous 3247C > T missense mutation. We searched for this insertion in 50 Japanese, 50 Korean and 50 Chinese control individuals, but none had it (Fig. 2a).

Although all 55 exons of *DYSF* were examined by the PCR-direct sequencing method, we could identify only one allelic mutation in four families (Table 1). No

Table 1 The clinical summary and mutations of the patients

Family no.	Patient no./sex	Age at onset (years)	Clinical phenotype	Exon	Mutation	Inheritance pattern
1	1a/M	20	MM	20	**2234G > A (G618R)**	Heterozygous
	1b/F	25		45	**5358C > G (T1662R)**	
2	2a/M	33	LGMD	32	**3817–8TG > AA**	Homozygous
	2b/F	11	MM		**(1148X)**	
3	3/F	12	MM	38	**4454T > C (C1361R)**	Heterozygous
				44	**5245delG(1633X)**	
4	4/F*	23	LGMD	42	**4887A > G (Y1505C)**	Heterozygous
5	5/F*	26	MM	37	**4376G > A (E1335K)**	Heterozygous
6	6a/M	60	High CK	27	**3247C > T (R958W)**	Homozygous
	6b/M	20	MM/LGMD			
	6c/M	18	MM			
7	7/M*	17	LGMD	37	**4376G > A (E1335K)**	Heterozygous
8	8/M	17	MM	29	**3483C > T (R1041C)**	Homozygous
9	9/M	19	MM	25–29	2885–3547del (Y838-R1058 del)	Homozygous
10	10/M*	17	LGMD	23	2573–7del (750X)	Heterozygous

M, male; F, female; MM, Miyoshi myopathy; LGMD, limb-girdle muscular dystrophy; CK, creatine kinase.

Bold text, novel mutation.

*families where only one allelic mutation was identified.

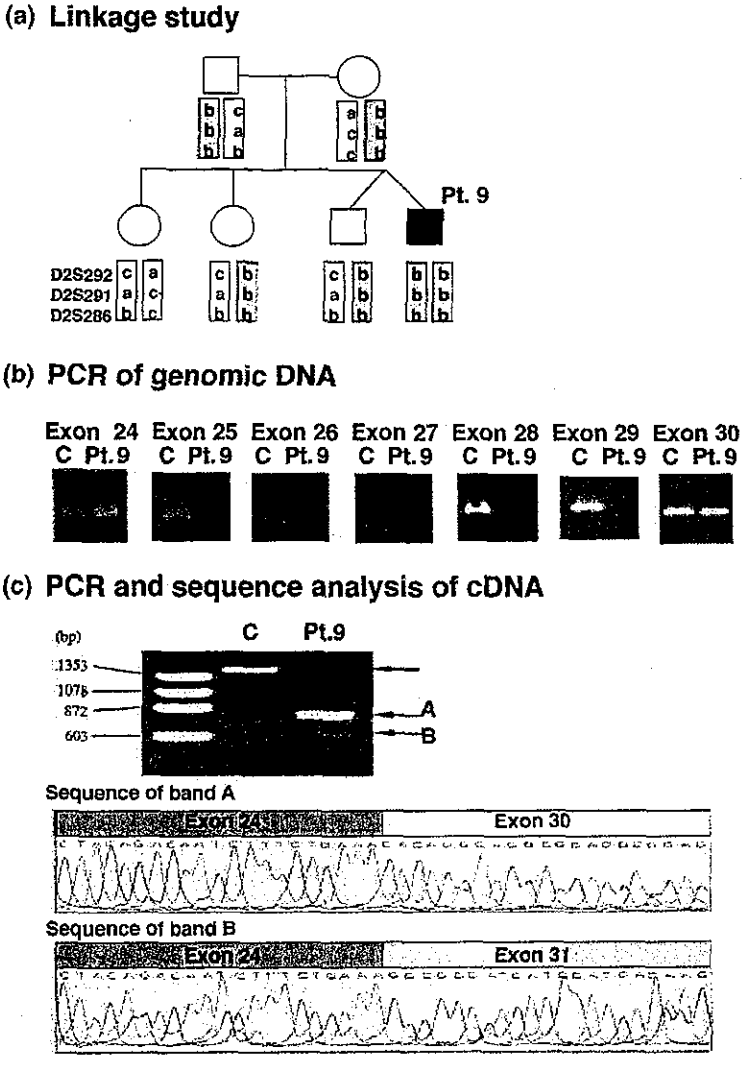

Figure 1 Large deletion of *DYSF* in a family (F9). (a) Haplotype analysis. Only one patient (patient 9) showed homozygous in three markers for chromosome 2p. (b) PCR of genomic DNA. In this patient, no amplified product was observed from exons 25 to 29. PCR products of the other exons were clearly amplified with the expected size. (c) RT-PCR. Two types of PCR products (A and B) were amplified using cDNA from biopsied muscle. Sequence analysis of these bands revealed deletions from exons 25 to 29 (band A) and from 25 to 30 (band B).

truncated transcript was amplified by RT-PCR in these four heterozygous families, either.

Discussion

Dysferlin is a FER-1 member protein and contains six putative C2 domains (Liu *et al.*, 1998a; Britton *et al.*, 2000), which can bind to phospholipids, inositol polyphosphates, Ca^{2+} and intracellular proteins (Nalefski and Falke, 1996; Rizo and Sudhof, 1998). The function of dysferlin is not yet known. However, it localizes to the plasma membrane of skeletal muscle and might have a role in membrane fusion (Anderson *et al.*, 1999; Matsuda *et al.*, 1999). Recently, Bansal *et al.* (2003) reported the possible involvement of dysferflin in the membrane-repair machinery in skeletal muscle. Mutations in *DYSF* cause different clinical phenotypes of muscular dystrophy and the distribution of affected muscles is different between patients, even in the same family. Some patients show onset in proximal muscles, while others show initial selective atrophy and weakness of calf muscles and are diagnosed as MM. However, muscle weakness and atrophy are progressive, and subsequently both proximal and distal muscles are involved in most of the patients.

In the present study, we performed mutation analysis on 14 Italian patients from 10 unrelated families who were clinically suspected of having LGMD or MM and showed a deficiency in the dysferlin protein by immunoblotting analysis. As *DYSF* on chromosome 2p13 contains 55 exons and encodes a 6911-bp mRNA (AF075575), the mutation screening is complex and time consuming. Furthermore, many polymorphisms have been reported. PCR-SSCP analysis is thought to